Food Hydrocolloids 172 (2026) 112154

Contents lists available at ScienceDirect

Food Hydrocolloids

journal homepage: www.elsevier.com/locate/foodhyd

High moisture extrusion based texturization and functional modulation of pea protein isolate through integration with cultivated beef

Vahid Baeghbali [a,b], Stephen R. Euston [c,d], Xi He [a,b], Manuela Donetti [e], Osama Maklad [f,b], Parag Acharya [a,b,*]

[a] Natural Resources Institute, Faculty of Engineering and Science, University of Greenwich, Medway Campus, Central Avenue, Chatham Maritime, Kent, ME4 4TB, UK
[b] Bezos Centre for Sustainable Protein, University of Greenwich, Medway Campus, Central Avenue, Chatham Maritime, Kent, ME4 4TB, UK
[c] Heriot-Watt University, Institute of Biological Chemistry, Biophysics and Bioengineering, School of Engineering & Physical Sciences, Edinburgh, EH14 4AS, UK
[d] University, Toronto, Department of Physics, Toronto Metropolitan, ON, M5B 2K3, Canada
[e] Ivy Farm Technologies, Oxford, UK
[f] School of Engineering, Faculty of Engineering and Science, University of Greenwich, Medway Campus, Central Avenue, Chatham Maritime, Kent, ME4 4TB, UK

ARTICLE INFO

Keywords:
Hybrid plant-based meat analogue
High moisture extrusion (HME)
Sustainable protein blend
Cultivated meat
Hybrid alternative protein
Plant protein texturization

ABSTRACT

The increasing global demand for meat can be sustainably leveraged by alternative protein, but the inferior quality of current plant-based meat analogues has somewhat disillusioned consumers. Small inclusion level of cultivated beef (CB) to bulk pea protein isolate in the high moisture extrusion (HME) showed a process unlock how to modulate the texture and instrumental sensory properties of the hybrid pea protein extrudates. Such novel co-extrusion delivered improved physicochemical and flavour properties as well as imparted distinct change in texture and microstructure. A comparison between hybrid pea protein extrudates with 10 % CB (*E*-PCB10) and 2 % CB (*E*-PCB2) showed a clear enhancement of the water holding (~16.7-fold) and oil holding (~67-fold) capacities in *E*-CPB10 and the instrumental sensory analyses also showed up to 30 % reduction of key off-flavour markers of pea protein in *E*-PCB10 along with reduction in bitterness and astringency. *E*-PCB10 and *E*-PCB2 exhibit different microstructure compared to *E*-PPI, and *E*-PCB10 showed increased hardness, resilience, cohesiveness and chewiness as well as the mechanical strength. The scanning electron microscopy of extrudates revealed that higher concentrations of cultivated beef disrupted the pea protein matrix and the laminar structure in *E*-PPI becomes less easy to discern in *E*-PCB2 and *E*-PCB10. The increasing percentage of CB leads to a more enhanced protein-protein cross-linking in *E*-PCB10. These findings demonstrated for the first time that an addition of as little as 2 % and 10 % of cultivated beef can modulate the texture and microstructure of pea protein extrudate. This could lead to a promising texturization process for plant protein via microstructure modulation, reducing off-taste, and enhancing functional features to develop high-quality, hybrid alternative protein-based meat analogue.

1. Introduction

Population growth, increased income and demand for protein rich diets has resulted in a surge in the global consumption of meat, which is expected to increase by 50 % or more by 2050 (Jang & Lee, 2024; Rueda & Scherer, 2023). Global livestock production is responsible for 14.5 % of the total anthropogenic greenhouse gas (GHG) emission and one third of current human-induced nitrogen emission (65 Tg N yr^{-1}), as well as contributing to 30 % of the biodiversity loss, 77 % of agricultural land usage, and 30 % of all water resources (Cheng et al., 2024; Clark et al., 2020; Humpenöder et al., 2022; Schiermeier, 2019; Smetana et al., 2023). To mitigate the impact of climate change on our food system and to sustainably deliver the future demand for protein, alternative protein sources should emerge as mainstream. The use of alternative proteins in innovative meat analogues should take centre stage as a contributor to decarbonization of the food system (Baig et al., 2024; Lurie-Luke, 2024; Malila et al., 2024; Surya Ulhas et al., 2023).

The choice of alternative protein sources has important implications for the development of meat analogues particularly the sensory and nutritional properties (Arora et al., 2023; Munialo, 2024).

* Corresponding author. Natural Resources Institute, Faculty of Engineering and Science, University of Greenwich, Medway Campus, Central Avenue, Chatham Maritime, Kent, ME4 4TB, UK.
E-mail address: p.acharya@greenwich.ac.uk (P. Acharya).

https://doi.org/10.1016/j.foodhyd.2025.112154
Received 2 August 2025; Received in revised form 11 October 2025; Accepted 21 October 2025
Available online 27 October 2025

High-moisture extrusion (HME) is so far the most established, cost-effective and scalable process to produce texturized plant protein for meat analogue (De Angelis et al., 2024; X. Zhang, Shen, et al., 2024a). Soy protein together with gluten is overwhelmingly used in current plant-based meat alternative (PBMA) formulation (Zhang, Zhao, et al., 2022b), however, over-dependency on imported soy may promote emissions, land use changes due to deforestation, large food miles etc., that can lead to up to 23 % increase in carbon emissions (Dreoni et al., 2022). Moreover, soy for human food is typically required to be certified GM-free and traceable (Oxford University Environmental Change Institute, 2021). Thus, by unlocking the functional potential of a diverse range of locally grown, under-utilized legume proteins, can potentially provide novel plant-based meat alternatives (Huamaní-Perales et al., 2024; X. Zhang, Zhang, et al., 2024b). Leveraging plant protein blends for future food has also been demonstrated (Jareonsin et al., 2024; Jiménez-Munoz et al., 2021; Schreuders et al., 2021).

The legume pea is a major protein containing crop having distinct advantages like lower environmental footprint, superior soil nitrogen fixation, health benefits, and functional properties which make it a compelling alternative (Shanthakumar et al., 2022; Wang, Kadyan, et al., 2022a). Various studies had shown application of HME to generate fibrous morphology using only pea protein (Barnés-Calle et al., 2024; Plattner et al., 2024; Zang et al., 2025) or combining it with other plant proteins like wheat gluten (Zhao et al., 2024), faba (Ferawati et al., 2021), oat (Gaber et al., 2023), chickpea (Webb et al., 2020) or microalgae like Chlorella (Sägesser et al., 2024). Pea protein isolate had also been co-extruded together with starch (Dahl et al., 2025), conventional meat (Pöri et al., 2023) and whey protein (J. Zhang et al., 2025a).

Despite recent advancements in plant-based meat alternatives, inferior taste and texture of the current products are a major barrier for market growth (Jang & Lee, 2024; Lindberg et al., 2024). Thus, functional and organoleptic qualities of the textured plant proteins must be improved to further drive consumers' acceptance of PBMA (Abdul Kareem et al., 2024; Anusha Siddiqui et al., 2023; Rubio et al., 2020).

Another emerging source of alternative protein is cell-based or cultivated meat production (Deliza et al., 2023; Pawar et al., 2023; Post et al., 2020; Riquelme-Guzmán et al., 2024). This has fundamental advantages of higher feed conversion rates (25 % vs 4 %) and a faster production cycle (~2 weeks vs. 3 years) than beef (Deloitte LLA, 2019; Warner, 2019). Although the innovation forecast for cultivated meat looks optimistic, the scalability is still a challenge and the production costs must decrease by 50 %–80 % to deliver the price parity with beef (Garrison et al., 2022; Hubalek et al., 2022).

It has been suggested that mixing of alternative protein sources can potentially solve the quality insufficiency of individual textured plant protein (Kaplan & McClements, 2025; Villacís-Chiriboga et al., 2025), but there is a clear knowledge gap in attempts to understand the texturization of plant protein in the presence of other types of alternative proteins.

There are studies combining bulk cultivated meat cells with ingredients from plants, bacteria, and algae including various types of binders to mimic the taste and texture of real meat (Lee, Kim, et al., 2023a). Besides, plant and fungus derived scaffolding materials (Bomkamp et al., 2022) have also been tested, for example, soy and pea proteins were investigated as hydrogel scaffolds for cultivated meat (An & Kim, 2024). In this study we explored the influence of a small amount of cultivated beef in texturization of pea protein isolate using HME (Flory et al., 2023; Ozturk & Hamaker, 2023), where the cultivated beef cells act as high-impact functional ingredient to modulate the overall texture and functions of pea protein extrudates. To the best of our knowledge, this is the first report of HME applied to the hybrid mix of plant protein and cultivated meat cells.

2. Materials and methods

2.1. Materials

Commercial food grade pea protein isolate (PPI) was obtained from BakeRite (Melton, UK) and Cultivated beef (CB) samples were supplied by Ivy Farm Technologies (Oxford, UK). Cultivated beef cells had 87.5 % moisture, 12.1 % protein and 0.32 % total fat (wet basis). PPI contained, on a dry matter basis, at least 87.3 % protein as well as 4.13 % of fat and had the moisture content of 8.30 % (wet basis).

2.2. Methods

2.2.1. Experimental design

The aim of this study was to assess the impact of the change in texture, microstructure upon high moisture extrusion of different ratios of cultivated beef (CB) added to pea protein isolate (PPI) as well as to assess the effect on sensory and other functional properties of the resultant hybrid extrudates. For the HME experiments, PPI (100 w/w %) was used as the control and for the partial replacement of PPI, the two hybrid formulations PCB2 (CB:PPI = 2:98 w/w) and PCB10 (CB:PPI = 10:90 w/w) were prepared by premixing CB at a concentration of 2 % w/w and 10 % w/w respectively with PPI powder. The HME of PPI, PCB2 and PCB10 resulted in production of extrudates *E*-PPI, *E*-PCB2 and *E*-PCB10 respectively having moisture content of 57.71 ± 0.16 %, 58.10 ± 0.21 % and 60.02 ± 0.15 %.

In this study, the effect of CB incorporation on water and oil holding capacities, specific mechanical energy (SME), texture, and flavour of *E*-PCB2 and *E*-PCB10 have been calculated using the following equations (1a) and (1b) which signify the change due to incorporation of 2 % and 10 % w/w CB respectively

$$\Delta 2\%\ \mathrm{CB} = (\mathrm{E} - \mathrm{PCB2}) - (\mathrm{E} - \mathrm{PPI}) \tag{1a}$$

$$\Delta 10\%\ \mathrm{CB} = (\mathrm{E} - \mathrm{PCB10}) - (\mathrm{E} - \mathrm{PPI}) \tag{1b}$$

For Δ2 % CB and Δ10 % CB values, the error was calculated using the pooled standard deviation (equation (1c)) the pooled SD was then normalized by dividing it by the mean of the reference group (*E*-PPI) and multiplying by 100 to express it as a percentage.

$$SD_{pooled} = \sqrt{\frac{SD_1^2 + SD_2^2}{2}} \tag{1c}$$

where SD_1^2 is the variance (standard deviation squared) of the first group (*E*-PPI) and SD_2^2 is the variance of the second group (*E*-PCB2 or *E*-PCB10). Relative error for each value was then calculated using on the following equation (1d):

$$\text{Relative error}\ (\%) = \left(\mathrm{SD}_{\mathrm{pooled}} \,/\, \mathrm{Mean}_{\mathrm{E-PPI}}\right) \times 100 \tag{1d}$$

2.2.2. High moisture extrusion process

Three extrusion trials with three repeats per trial were conducted using a co-rotating twin-screw extruder (Process 11 Hygienic, Thermo Fisher Scientific, Karlsruhe, Germany) with screw diameter of 11 mm, the length to diameter (L/D) ratio of 40 and using screw speed of 400 rpm. The extruder barrel consists of eight-barrel sections (seven screw sections and a die adapter) which can be heated and cooled independently, and the barrel temperature profile of the sections was set at 40, 60, 80, 100, 130, 150, 140, 120 °C towards the die respectively. The first barrel element is connected to a gravimetric feeder for adding protein/protein blend (flow rate used: 3.7 g/min) and deionised water was dosed at the third barrel element using a peristaltic pump from Cole Parmer (Masterflex L/S, Vernon Hills, IL, USA) at a flow rate of 4.8 ml/h for PPI, and PPI + 2 % CB as well as 4.7 ml/h for PPI + 10 % CB. The feed flow rate and water flow rate were selected based on preliminary tests to get a consistent fibrous texture in the product. The die adapter is 32 mm long

and provides a transition from the barrel element to the attached slit cooling die (125 × 19 × 4 mm) which was cooled constantly at 20 °C using circulating deionised water temperature controlled by an Accel 500 chiller (Thermo Fisher Scientific, US). Samples were vacuum packed, sealed and kept at 4 °C in a refrigerator until analysis.

The SME was calculated as described by Lee, Kim, et al. (2023b) by using equation (2), using the values of torque, screw speed, and mass flow rate at steady extrusion state. The torque percentage was displayed on the extruder screen with the maximum nominal torque of 12 Nm for the used extruder. The mass flow rate was calculated based on the powder and water flow rates at the steady processing state per minute. Measurements were conducted in triplicate.

$$SME(kJ/kg) = \frac{2\pi \times n \times T \times P}{100M} \quad (2)$$

where n is the screw speed (400 rpm); T is the motor torque (N·m); P is the torque percentage (100); and M is the mass flowrate (g/min). The average torque for PPI, PCB2 and PCB10 was 0.96 Nm, 1.08 Nm and 0.72 Nm respectively and the die pressure for these samples was 10 bar, 13 bar and 8 bar respectively.

2.2.3. Protein, total fat and moisture analysis and water and oil holding capacities

2.2.3.1. Protein, total fat and moisture analysis. Total protein content of the ingredients was measured using a LECO® FP828 nitrogen analyser (LECO, St. Joseph, MI, USA) and a conversion factor of 6.25 (Pöri et al., 2023). Moisture content (% w/w) was measured using a microwave and infrared gravimetric moisture analyser (SMART 6; CEM Corporation, NC, USA). The total fat content was determined using a nuclear magnetic resonance fat analyser (Oracle, CEM Corporation, NC, USA). Both moisture and fat determination was performed according to the AOAC 2008.06 official method (Leffler et al., 2008) which remains current in the 22nd Edition (2023)of AOAC Official Methods of Analysis (Latimer, 2023).

2.2.3.2. Water and oil holding capacities. Extrudates were freeze-dried, milled, and sieved through a 250 μm mesh prior to water-holding capacity (WHC) and oil-holding capacity (OHC) analysis. This step standardizes sample geometry for reproducibility and aligns with established extrusion literature, which routinely quantifies WHC/OHC on dried or powdered extrudates (Singh et al., 2025; Snel et al., 2023; Yu et al., 2025). Although high-moisture extruded proteins are typically consumed intact, WHC or OHC values from dried powders provide a controlled measure of the intrinsic ability of the protein network to retain water and oil, independent of free moisture. Briefly 1 g of the ingredients (or freeze dried and powdered extruded product) was weighed into 50-mL centrifuge tube and 10 g of deionised water (for WHC) or refined sunflower oil (for OHC) was added to it. The tube caps were then closed, and they were vortexed for 10s every 5 min for 30 min using a vortex shaker (Cole-Parmer V-200 Stuart Vortex Mixer, UK). Then tubes were centrifuged for 20 min at 1500×*g* for (Multifuge X pro, Thermo Fisher Scientific, USA). After centrifugation the remaining pellet was weighed and WHC and OHC were then calculated using the following equations:

$$WHC = \frac{W_f - W_i}{W_i}$$

$$OHC = \frac{W_f - W_i}{W_i}$$

where W_i is to the sample's initial weight, and W_f is the pellet's final weight (Singh et al., 2025).

2.2.4. Protein characterisation

2.2.4.1. Surface hydrophobicity and intrinsic fluorescence. Surface hydrophobicity of *E*-PPI, *E*-PCB2 and *E*-PCB10 was determined using 8-anilino-1-naphthalenesulfonic acid (ANSA) as a fluorescent probe (2.4 mM) applying methods according to Saricay et al. (2014) with minor adjustment. Sample dispersions (0.12 mg dry matter/mL) were prepared in 10 mM phosphate buffer (pH 7.0). ANSA solution (10 μL) was added to 1 mL of each dispersion, and fluorescence intensity was measured using a Varioskan™ LUX microplate reader (Fisher Scientific). The excitation wavelength was at 385 nm, and the emission was scanned from 410 to 620 nm at 10 nm intervals. After blank subtraction, the relative surface hydrophobicity (H_0) was calculated as the integrated area under the fluorescence emission curve between 410 and 620 nm (Jiang et al., 2024; Li & Li, 2023; Saricay et al., 2014). Intrinsic fluorescence was measured on the same sample dispersions to evaluate protein tertiary structure using the method reported by Varejão and Reverter (2023, pp. 229–241) with minor adjustment. Fluorescence spectra were recorded using the same instrument with an excitation wavelength of 285 nm and emission scanned from 310 to 410 nm at 10 nm intervals. After blank subtraction, spectra were analysed for emission maxima and intensity changes, which indicate conformational alterations (Varejão & Reverter, 2023, pp. 229–241).

2.2.4.2. Protein–protein interactions. Protein–protein interactions in the extrudates were analysed using the sequential extraction method described by Zhang et al. (2025b) with slight modifications. Ground extrudate samples (0.05 g) were dispersed in 10 mL of following extraction buffers targeting different interaction types.

- Ionic bonds: 0.1 M, pH 7.5 phosphate buffer saline (PBS)
- Hydrophobic interactions: 17.3 mM SDS in PBS (P + S)
- Hydrogen bonding (H-bonding): 8 M urea in the PBS (P + U)
- Hydrophobic and covalent interactions: 17.3 mM SDS in P + U (P + S + U)
- Disulfide bonds: 50 mM dithiothreitol (P + S + U + D)

Each extraction was performed by incubating at 1 h at 30 °C with frequent vortexing, followed by centrifugation at 8000×*g* for 15 min. The protein content in each supernatant was determined using Pierce™ Modified Lowry Protein Assay Kit (Thermo Fisher Scientific) at 750 nm and expressed as a percentage ratio of total extractable protein to the total sample weight (Zhang et al., 2025a).

2.2.5. Texture analysis

A TA.XT.Plus Texture Analyser (Stable Micro Systems, Godalming, England) was used for the following texture analysis tests.

2.2.5.1. Texture profile analysis (TPA). For the texture profile analysis (TPA), the extrudate samples (*E*-PPI, *E*-PCB2 and *E*-PCB10) were cut into rectangles of 20 × 20 mm and a height of 4 mm. Samples were compressed twice with a 40 mm aluminium cylinder probe to 50 % of the original height with a speed of 5 mm s^{-1} and a waiting time in between the two compressions of 5s. Samples were measured in triplicate. The peak maximum force at first compression was taken as the hardness. A 30 kg load cell was used for this test.

2.2.5.2. Cutting test and extensibility measurement. Cutting tests to measure extent of fibre formation (anisotropy/degree of texturization) were performed in both parallel and perpendicular directions to the rotational shear flow. Samples were cut into 20 × 40 mm pieces. Height was 4 mm. Samples were cut up to 75 % of their initial height with a Mullenet-Owenz Razor Shear Blade (A/MORS) with a test speed of 1 mm s^{-1}. The blade width was 10 mm. The razor blade shear force max (cutting force in N) was measured. Degree of texturization (DT) was

calculated as the ratio between cutting force in parallel ($F_{||}$) and perpendicular directions($F_{\perp}$): $DT = F_{||}/F_{\perp}$.

Resistance to extension was measured using miniature tensile grips and a 5 kg load cell was used. The test speed was 1.0 mm s^{-1} and the distance was 50 mm. Resistance to extension was the peak force (g) at the point the sample raptured (Stable Micro Systems Ltd, 2023.

2.2.5.3. Large Amplitude Oscillatory Shear (Laos) measurements. Large-amplitude oscillatory shear (LAOS) is a widely used technique for examining the nonlinear viscoelastic behaviour of materials. Unlike linear viscoelastic tests, the resulting stress response is not purely sinusoidal. Instead, the asymmetric stress signal can be expressed as a combination of sinusoidal components, beginning with the fundamental testing frequency and extending to odd multiples of that frequency, known as higher harmonics. Each higher harmonic possesses its own phase angle and provides insights into the material's molecular structure. LAOS data are often represented as parametric stress–strain plots, known as Lissajous–Bowditch curves. These curves typically form S-shaped loops that reflect viscoelastic behaviour, where the loop's width corresponds to the phase angle (Hyun et al., 2011; Liu et al., 2024). Nonlinear viscoelastic properties of the extrudates were evaluated using a Discovery HR-20 rheometer (TA Instruments, New Castle, DE, USA) equipped with a 40-mm parallel plate cross-hatched geometry. Samples were equilibrated at 20 °C for 10 min before testing. The samples were subjected to a 2.5 N fixed normal force and transient sinusoidal deformation at 22 different strain levels ranging from 0.01 % to 100 % at a frequency of 1 Hz.

2.2.6. Microstructure analysis

2.2.6.1. Scanning electron microscopy (SEM) methodology. Samples (approximate dimensions 2x2x4mm) of the extruded composite samples were cut across and along the axis of extrusion. The samples were then mounted on a sample holder and placed in the sample chamber of a Quanta FEG 650 scanning electron microscope (Thermofisher, UK). Visualization was carried out in low vacuum mode, with no further preparation of the sample, by evacuating the sample chamber to 110 Pa (0.825 Torr) over 5 min and viewing under a water vapor atmosphere. Drying out of the sample did occur under these conditions, but samples were removed from the chamber after visualization and inspection revealed no obvious and significant changes in structure before and after exposure to the vacuum.

2.2.6.2. Confocal microscopy. Samples (approximate dimensions 2x2x4mm) of the extruded composite samples were cut across axis of extrusion. Staining was carried out in a metal cell chamber with a coverslip bottom with a 10 mg/mL phalloidin-ATTO752 in water solution (ThermoFisher, UK, excitation wavelength 728 nm, emission wavelength 751 nm) and a 10 mg/mL Hoescht 33342 (ThermoFisher, UK, excitation wavelength 361 nm, emission wavelength 486 nm) stock solution diluted 1:1000 in water. Samples were incubated for 30 min in the dark in a 1:1 mixture of both stains that was sufficient to cover the sample. Imaging was carried out using a Leica SP8 inverted confocal microscope with 20x water immersion lens without removal of the staining solution. Phalloidin binds to and can be used to visualize and localise actin filaments. Hoescht 33342 is a nucleic acid stain that binds to double stranded DNA and can be used to visualize cell nuclei. We used the natural fluorescence of the protein when excited at 488 nm to visualize the protein structure.

2.2.7. Taste analysis

The samples were analysed for bitterness, astringency and umami taste as well as the bitterness and umami after tastes using an electronic taste sensing system (TS6000A, Insent Intelligent Sensor Technology Inc, Fukuoka prefecture, Japan) using a method described by Feng et al. (2025) with some modifications. Briefly the extruded samples were mixed with 10 times deionised water, dispersed using a Thermomix for 2 min at 5000 rpm, and then left at 4 °C for 4 h. Then the dispersions were centrifuged at 4 °C and 8000×*g* for 20 min, and the supernatants were taken for the taste analysis (Feng et al., 2025). All measurements were carried out in triplicates.

2.2.8. Flavour analysis

The aroma active volatile compound analysis has been performed using Centri-GC × GC-BenchTOF2 instrument (SepSolve). 2g of each minced extrudates *E*-PPI, *E*-PCB2 and *E*-PCB10 have been placed into 20 mL headspace vial having up to four replicates. The vials were incubated at 50 °C for 10 min and then the HiSorb extraction, using Divinylbenzene/Carbon wide range/Polydimethylsiloxane (DVB/CWR/PDMS), was taken place at 50 °C for 30 min with agitator speed of 350 rpm. The HiSorb probe was desorbed at 250 °C, and analytes were introduced onto trap and then desorbed in a 10:1 split mode. The GCxGC configuration consisted of the 1st polar column: WAX-HT column (20m × 0.18 mm × 0.18 μm) and the 2nd mid-polar column: BPX50 column (2.5m × 0.25 mm × 0.1 μm). The oven temperature ramp was programmed as follows: 40 °C held for 2 min; 4 °C/min to 250 °C and then held for 5min. The INSIGHT-flow modulator system was employed, and modulation period was 3.5 s with 175ms flush time. Helium was used as carrier gas at a flow of 0.5 mL/min for the 1st column and 20 mL/min for the 2nd column after the INSIGHT-flow modulator then 4 mL/min from detector splitter to the TOFMS. The transfer line and ion source temperature were set to 250 °C. TOF MS was operated at scan rate of 50 HZ in the mass range m/z 33–500 and using a tandem ionisation mode of 70eV and 14eV. The ChromSpace software was used for the data acquisition and processing. Library searching was performed using the NIST and WILEY library with EIC mode for the target compounds peak area extraction.

2.2.9. Statistical analysis

All the processing and analyses were carried out in triplicates and one-way analyses of variance (ANOVA) was used to determine the significant differences between three formulations ($p < 0.05$). R software (version 4.4.2, R Foundation for Statistical Computing, Vienna, Austria) was used for the statistical analysis. Multivariate data analysis was performed using averaged absolute values of measured parameters (hardness, adhesiveness, resilience, cohesiveness, springiness, gumminess, chewiness, work of shear/toughness, firmness, razor blade shear force max, razor blade shear energy, DT, resistance to extension, extensibility, SME, WHC, OHC, hexanal, 2-pentylfuran, 1-octen-3-ol, 2,4-decadienal, bitter, astringent, umami) which were introduced into SIMCA 17.0 (Umetrics, Umeå, Sweden) software, centring and unit variance scaling was performed prior to the principal components analysis (PCA). The HCA plot calculated with Ward's minimum variance method and sorted by size.

3. Results and discussions

3.1. Functional properties of hybrid pea protein extrudates

The moisture content, water-holding capacity (WHC) oil holding capacity (OHC) and specific mechanical energy (SME) are summarized in Table S1. The change in functional properties of extrudate reflects the degree of texture and microstructure modifications achieved during extrusion cooking. Both WHC and OHC increased with the increasing CB content in the pea protein extrudate, and 10 % w/w CB incorporation showed ~16.7 and ~67.6 fold increase of WHC and OHC respectively compared to 2 % w/w CB addition (Fig. 1A and B). The SME represents the energy input from driver motor into raw materials to be extruded and is related to the viscoelastic properties of extrudate (Schmid et al., 2022). The addition of CB to PPI influenced the SME and with higher amount of CB in *E*-PCB10 showed lowest energy input which signifies a more viscoelastic behaviour (Fig. 1C). While WHC and OHC

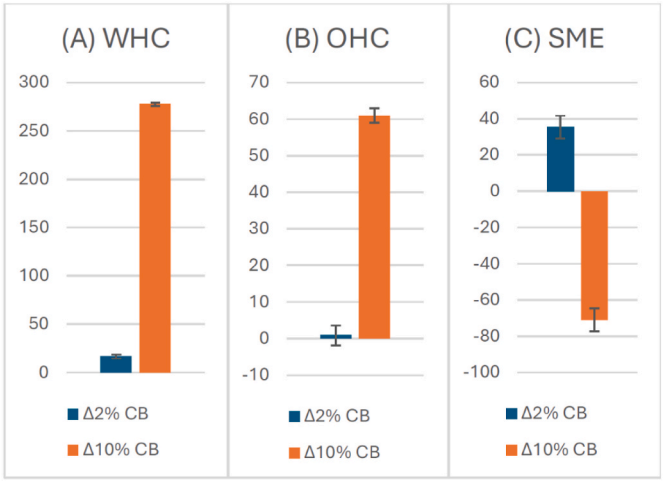

Fig. 1. *The changes in water-holding capacity (WHC; Panel A), oil holding capacity (OHC; Panel B) and specific mechanical energy (SME; Panel C) due to incorporation of 2 % w/w and 10 % w/w of CB into the pea protein for co-extrusion. The measured values of WHC, OHC and SME for extrudates E-PPI, E-PCB2 and E-PCB10 were* used (see Table S1) to calculate effect of 2 % w/w CB (Δ2 % CB) and 10 % w/w CB (Δ10 % CB) by using equations 1a and 1b (*see the section 'experimental design'*).

improvements coincide with microstructural densification, these changes likely result from multiple factors, including enhanced protein–protein interactions and compositional effects, rather than microstructure alone.

3.2. Protein characterisation of extrudates

3.2.1. Surface hydrophobicity and intrinsic fluorescence

The ANSA fluorescence probe reports the accessibility of hydrophobic patches on protein surfaces; increased signal reflects exposure of non-polar domains that typically emerges upon unfolding or partial denaturation, whereas subsequent aggregation or crosslinking can rebury these hydrophobic residues and reduce apparent surface hydrophobicity. High-moisture extrusion (HME) drives thermo-mechanical unfolding of pea globulins (11S legumin, 7S vicilin), followed by intermolecular crosslinking upon cooling. Incorporating CB has profound effect on the denaturation and concomitant increase of surface hydrophobicity in pea protein extrudates (see Fig. 2). Hybrid extrusion studies have shown that adding animal-derived proteins to plant matrices significantly modifies protein conformation and surface properties. Pöri et al. (2023) demonstrated that co-extrusion of pea protein with minced beef increased protein denaturation and altered network structure, consistent with greater exposure of hydrophobic domains during extrusion processing. (Osen et al., 2015; Y. Zhang & Xiao, 2025b).

The intrinsic fluorescence study (Fig. 3) clearly highlighted a loss of tertiary structure in order of *E*-PCB10 ≫ *E*-PCB2 > *E*-PPI. Intrinsic fluorescence spectra (310–410 nm) for all extrudate samples exhibited a consistent emission maximum at ~330 nm, with no detectable red or blue shift across treatments (Fig. 3). This indicates that the overall polarity of the tryptophan microenvironment remained broadly unchanged, suggesting limited large-scale tertiary unfolding during HME. However, fluorescence intensity at 330 nm decreased progressively from *E*-PPI to *E*-PCB2 and *E*-PCB10, implying increased quenching or burial of Trp residues within aggregated domains with increasing CB upon HME. Such intensity reduction is commonly associated with protein–protein interactions and network consolidation, where aromatic residues become less solvent-accessible or experience enhanced static/dynamic quenching (Xiao et al., 2025). These findings go hand in hand with the observed microstructural transition toward a denser, cohesive network in *E*-PCB10 (Fig. 7) and the lower SME recorded during extrusion, supporting the hypothesis that 10 % cultivated beef incorporation promotes stronger intermolecular associations rather than extensive unfolding of pea globulins (Lampinen et al., 2014; Varejão & Reverter, 2023, pp. 229–241).

3.2.2. Protein–protein interactions

High-moisture extrusion (HME) unfolds plant proteins, exposing reactive thiols and hydrophobic domains that promote new crosslinks such as disulfide bonds, resulting in a denser, water-retentive network (Muhialdin et al., 2024; Zhang et al., 2025a). Jiang et al. (2024) confirmed that HME significantly increases disulfide bond formation in pea protein systems, reinforcing the role of covalent crosslinking in structural consolidation. Incorporating cultivated beef (CB) amplifies this effect by introducing additional proteins that co-gel with pea proteins, strengthening the matrix and immobilising more water. Myofibrillar proteins (actin, myosin) from CB are highly effective at water binding and emulsion stabilisation, and upon cell lysis during extrusion, these proteins can crosslink with pea proteins, enhancing both water and lipid retention (Pöri et al., 2023; Villacís-Chiriboga et al., 2025). Furthermore, phospholipids and membrane proteins released from CB act as interfacial agents, reducing oil–water interfacial tension and stabilising fat droplets, which explains the marked increase in oil-holding capacity in hybrid extrudates (Pöri et al., 2023). Extracellular matrix polysaccharides (e.g., hyaluronan) from CB, being highly hydrophilic,

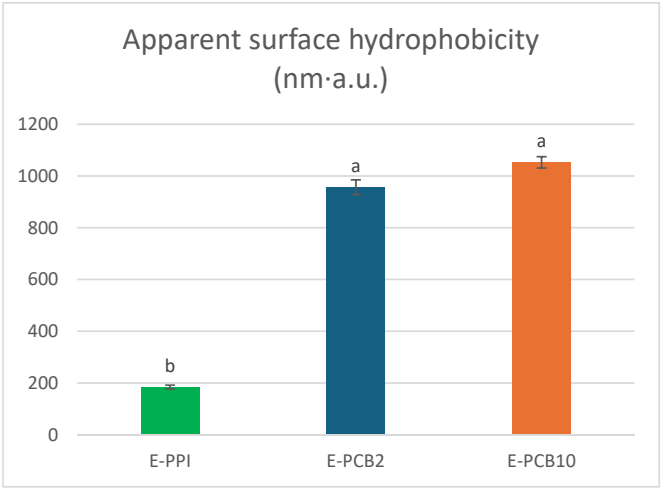

Fig. 2. Relative surface hydrophobicity (nm·a.u.) Different letters indicate significant differences (P < 0.05).

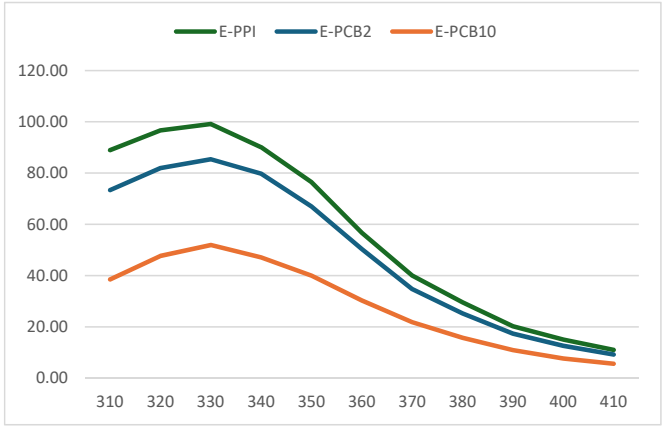

Fig. 3. Intrinsic fluorescence spectera for *E*-PPI, *E*-PCB2 and *E*-PCB10 (excitation wavelength of 285 nm).

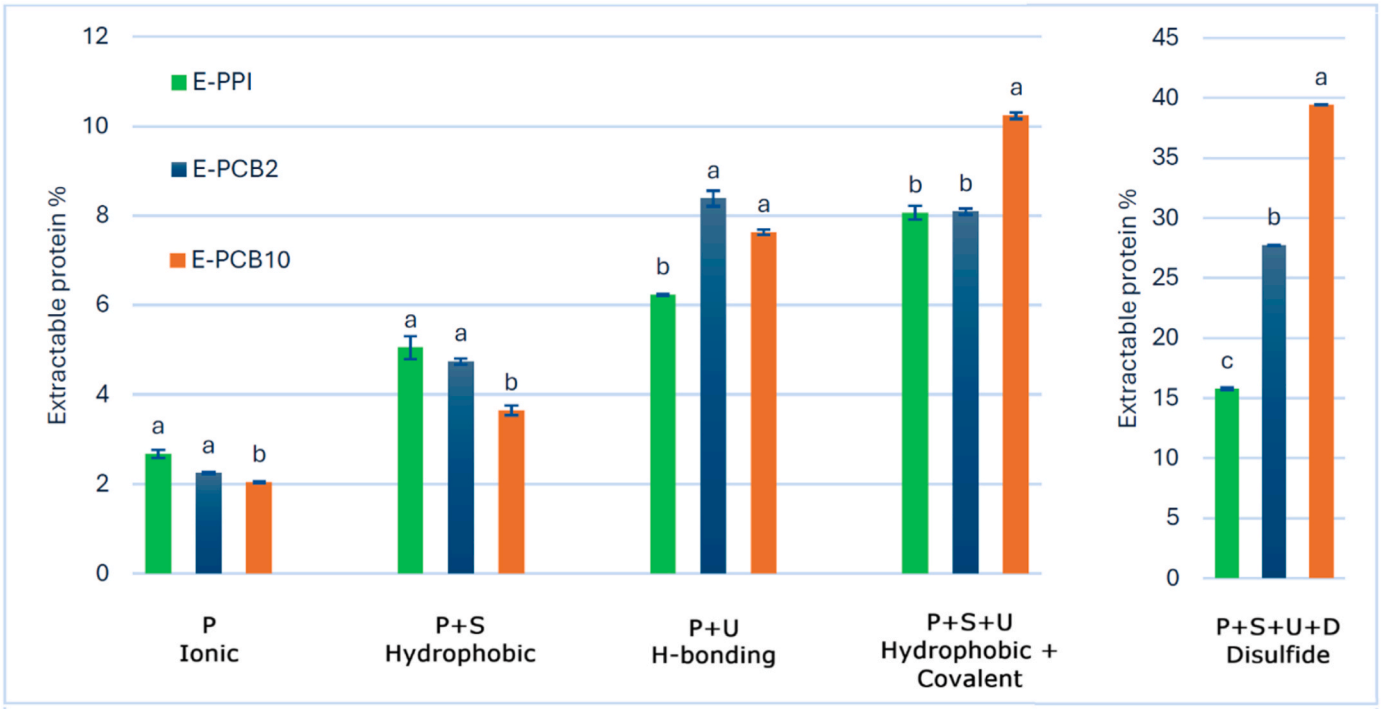

Fig. 4. The percent extractable protein using different extraction solvents: P: 0.1 M, pH = 7.5 Phosphate buffer saline (PBS); P + S: 17.3 mM SDS added to PBS; P + U: 8 M urea added to the PBS; P + S + U: 17.3 mM SDS added to P + U; P + S + U + D: 50 mM DTT added to P + S + U. Different letters indicate significant differences ($P < 0.05$). The percent extractable protein values are proportional to different protein-protein interactions as designated in the graph (see section 2.2.4.1. for details).

can increase viscosity and water retention, while cellular ions (K^+, Na^+, Cl^-) influence pea protein gelation through charge screening and salting-in/out effects, further modifying network porosity and hydration (Villacís-Chiriboga et al., 2025; J. Zhang et al., 2025b).

The dominant forces during and after extrusion vary with formulation and process conditions. Xiao et al. (2025) reported that disulfide-mediated crosslinking is the primary force maintaining fibrous integrity post-extrusion, while (Osen et al., 2015) identified hydrogen bonding as dominant during extrusion, with disulfide bonding playing a secondary role. These findings underscore that interaction hierarchies are dynamic and influenced by moisture, shear, and ingredient composition (Schmid et al., 2022). As CB content increases, more disulfide crosslinks formed in extrudates in order of *E*-PCB10 > *E*-PCB2 > *E*-PPI. This is primarily due to higher levels of sulfur-containing amino acids in CB proteins than in PPI, which promotes enhanced thiol–disulfide exchange during extrusion. Additionally, the HME process can break intramolecular disulfide bonds in CB, converting them into sulfhydryl groups that subsequently form intermolecular disulfide bonds with PPI, further strengthening the hybrid network (Jiang et al., 2024; Xiao et al., 2025). Proteins from different sources exhibit distinct denaturation and polymerisation behaviours, which explains the structural differences observed between pea-only and hybrid extrudates (Xia et al., 2022). Considering the microstructural consolidation and textural reinforcement in *E*-PCB10 (higher hardness, toughness/extensibility; cohesive network with loss of discrete fibrils) are indicative of greater covalent crosslink density and more extensive hydrophobic packing-precisely the pattern expected to shift solubility toward the SDS + urea + DTT step. Thus, complementary solvent extraction studies on extrudates modulating interactions with DTT (disulfide disruption), SDS (hydrophobic shielding) and urea (hydrogen bond disruption) confirm that disulfide bond formation dominates texturized PPI strength, with hydrophobic and electrostatic forces playing auxiliary roles - mirroring the interaction hierarchy inferred here for the CB added to PPI (Muhialdin et al., 2024). These cooperative interactions explain the dramatic WHC/OHC increases and reduced off-flavour release in *E*-PCB10, both of which are common outcomes of denser, more hydrophobically integrated networks with greater capacity to bind and retain water, oil, and aroma compounds (Totosaus et al., 2002; Villacís-Chiriboga et al., 2025).

3.3. Modulation of textural properties

3.3.1. Textural profile analysis, extensibility and cutting tests

The major challenge of developing plant-based meat analogues revolves around mimicking tactile properties of conventional meat products like mouthfeel, chewiness, cohesiveness or springiness etc (Alam et al., 2024). Texture is the sum of different physical properties like hardness, chewiness, resilience etc. which correlate with the mechanical deformation of food physical structures. The texture profile analysis (TPA) showed (Fig. 5A) that addition of CB to pea protein extrudate increases resilience, cohesiveness, and adhesiveness, but hardness, chewiness and gumminess first decrease for *E*-PCB2 (at 2 % w/w CB inclusion level) and then increases for *E*-PCB10 (at 10 % w/w CB inclusion level). Extensibility and firmness also showed marked improvement in *E*-PCB10 (Fig. 5B–D), indicating a denser and more mechanically robust structure. Overall, there is a significant difference in the textural properties of the *E*-PCB10 versus *E*-PCB2 when compared to the *E*-PPI (Fig. 5 and Table S2 in Supplementary information). The decreasing hardness in *E*-PCB2 implies that addition of CB could have created a softer texture by interacting with rigid cross-linking structure of pea protein. However, with increasing CB, strong gel formation enhances the structural integrity of *E*-PCB10, and such protein-protein network consolidation is supported by increasing S-S mediated intermolecular cross-linking found in *E*-PCB10 (Fig. 4). There is a clear increase of mechanical strength of pea protein extrudate due to addition of 10 % w/w CB compared to 2 % w/w CB showcasing higher toughness, firmness and extensibility (Fig. 5C). A wet-spinning-based texturization study by Kim et al. (2024) also indicated an antagonist texture effect

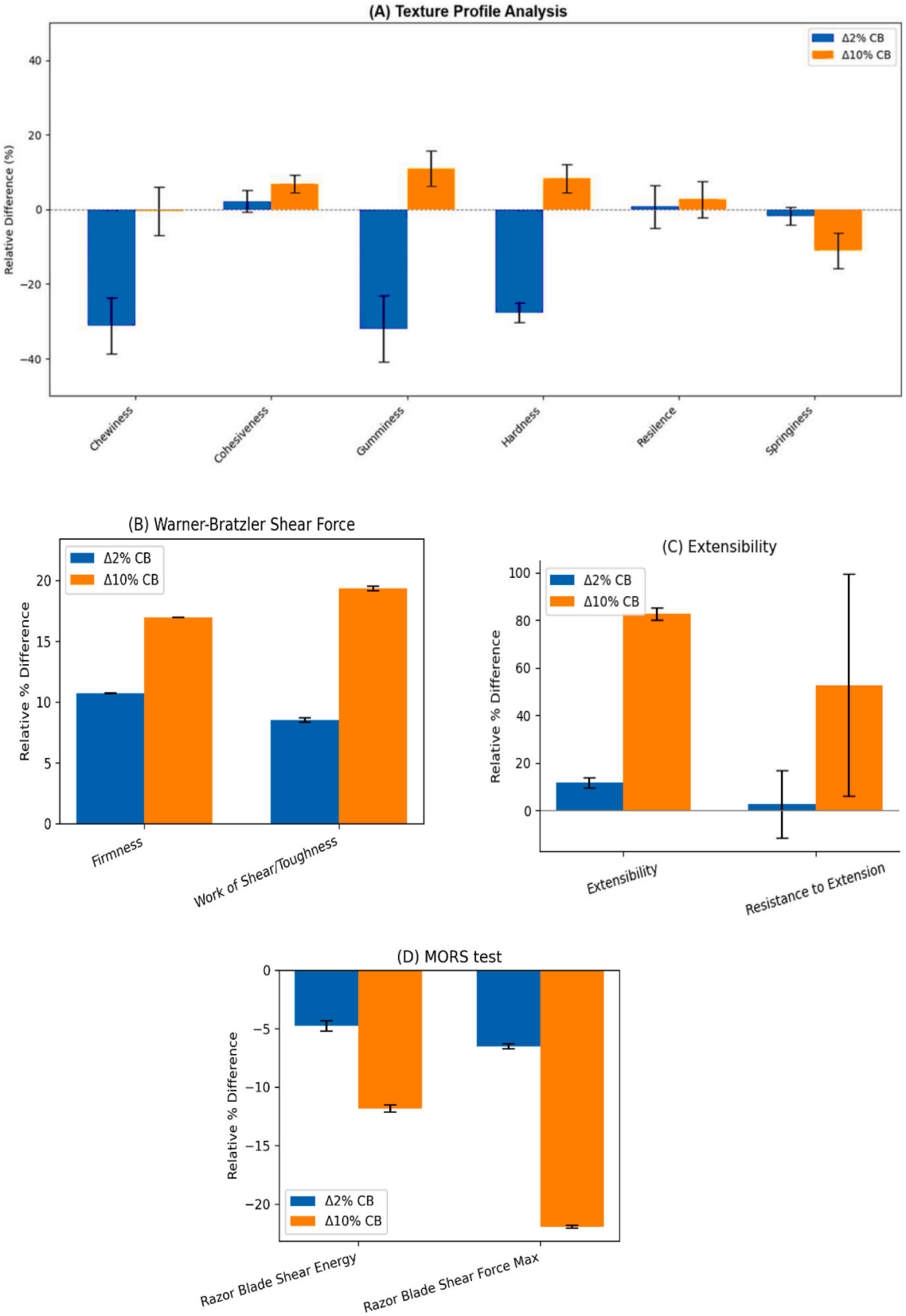

Fig. 5. (A) *Textural properties obtained from the Texture Profile Analysis (TPA),* (B) *Warner-Bratzler (WB) Shear Force (Meat Tenderness), (C) Extensibility, and (D) Meullenet-Owens Razor Shear Blade (MORS)* tests. All graphs are based on equation (1a) (i.e. effect of 2 % CB addition, Δ2 % CB) and equation (1b) (i.e. effect of 10 % CB addition, Δ10 % CB) as described under the section experimental design. The texture parameters for extrudates E-PPI, E-PCB2 and E-PCB10 are taken from Table S2 and used in equations 1a and 1b.

when low concentration of cultivated chicken cells was added to a blend of pea and wheat proteins, but with increasing concentration of cultivated chicken cells, further cross-linking enabled a firm and more cohesive texture (Kim et al., 2024).

3.3.2. *Large Amplitude Oscillatory Shear (Laos) measurements*

As two proteins are mixed and heated to form a gel, three interaction scenarios are possible; (a) Compatibility when both proteins co-assemble into an integrated gel network, enhancing water retention and mechanical strength. (b) Semi-compatibility when one protein forms the primary gel network, while the other interacts with it, modifying rigidity and elasticity. This often increases hardness and water retention, though effects are protein dependent. (c) Incompatibility when proteins form separate networks or distinct gel domains, leading to phase separation, weakened mechanical properties, and heterogeneous microstructure. Previous studies illustrate these behaviours. Sun and Arntfield (2012) reported that adding pea protein isolate (PPI) to myofibrillar protein gels reduced G′ and gel strength at 4 % total protein, suggesting incompatibility. Conversely, in meat batters and patties, PPI addition increased gel hardness, indicating compatibility (Lin & Barbut, 2024; Shen et al., 2022; Zhu et al., 2022). These discrepancies may arise from differences in meat protein type (myofibrillar vs. sarcoplasmic), protein ratios, or overall concentration.

The LAOS results suggest either compatibility or semi-compatibility between the proteins studied, as evidenced by changes in nonlinear parameters (e.g., strain stiffening and third harmonic intensities) that indicate network integration rather than phase separation. This interaction likely contributes to the observed improvements in texture and water retention in *E*-PCB10.

Fig. 6 shows the amplitude sweep (6a) and Lissajous–Bowditch curves (6b-d). The amplitude sweep results (Fig. 6a), where the storage modulus (G′) of all samples (*E*-PPI, *E*-PCB2, and *E*-PCB10) remains relatively stable at low strain amplitudes, indicating a predominantly elastic response within the linear viscoelastic region. However, as strain increases, G′ declines sharply, marking the onset of structural breakdown and transition toward nonlinear behaviour. Among the samples, *E*-PCB10 exhibits the highest G′ across the strain range, reflecting a denser and more cohesive network compared to *E*-PPI and *E*-PCB2 (Badii et al., 2016; Klost & Drusch, 2019; Moakes et al., 2015). Panels (b–d) illustrate LAOS behaviour at increasing strain amplitudes; Fig. 6b shows the Linear region (0.06 % strain): Lissajous–Bowditch loops remain nearly elliptical, and the stress response is close to sinusoidal, signifying minimal nonlinearity and dominance of elastic behaviour. Nonlinear region (4 % strain): Loops widen and distort, revealing intra-cycle strain stiffening and viscous contributions, indicative of network rearrangement and partial junction slippage (Fig. 6c). Deep nonlinear region (25 % strain): Loops become markedly asymmetric with pronounced stress overshoot during loading and delayed unloading, characteristic of yielding and strain-induced restructuring (Fig. 6d) (Erturk et al., 2023; Ewoldt & McKinley, 2010; Hyun et al., 2011).

The denser, cohesive network and higher mechanical strength of *E*-PCB10 relative to *E*-PPI or *E*-PCB2 suggest three LAOS signatures are likely to co-occur:

The progressive transition from linear to nonlinear response highlights the structural resilience of *E*-PCB10, which delays yielding and maintains greater elastic integrity under large deformations. These nonlinear fingerprints-elastic strain stiffening, reduced viscous dissipation, and delayed onset of nonlinearity-correlate with improved textural properties and water retention in the corresponding gels (Y. Wang & Selomulya, 2022b; Yazar et al., 2019).

The LAOS results have demonstrated delayed yielding, strong strain stiffening, and cohesive elastic loops for *E*-PCB10, suggesting compatibility in gel formation, where the proteins interact synergistically to reinforce the network rather than phase-separate. This interpretation aligns with studies reporting improved gel hardness and water retention in compatible systems (Lin & Barbut, 2024; Shen et al., 2022), contrasting with incompatibility cases where G′ decreases with added plant protein (Sun & Arntfield, 2012).

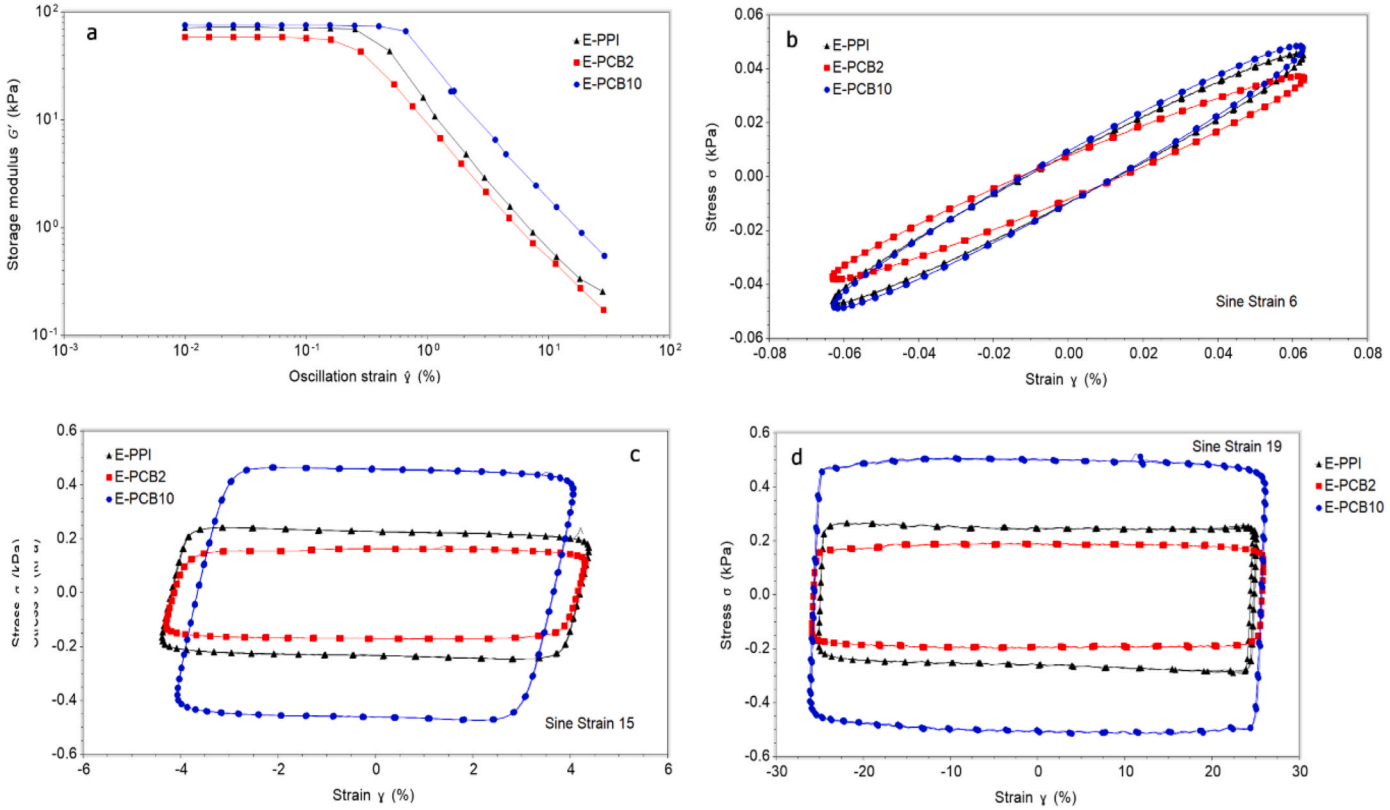

Fig. 6. Amplitude sweep (a) and Large Amplitude Oscillatory Shear (LAOS) Lissajous–Bowditch curves (b–d).

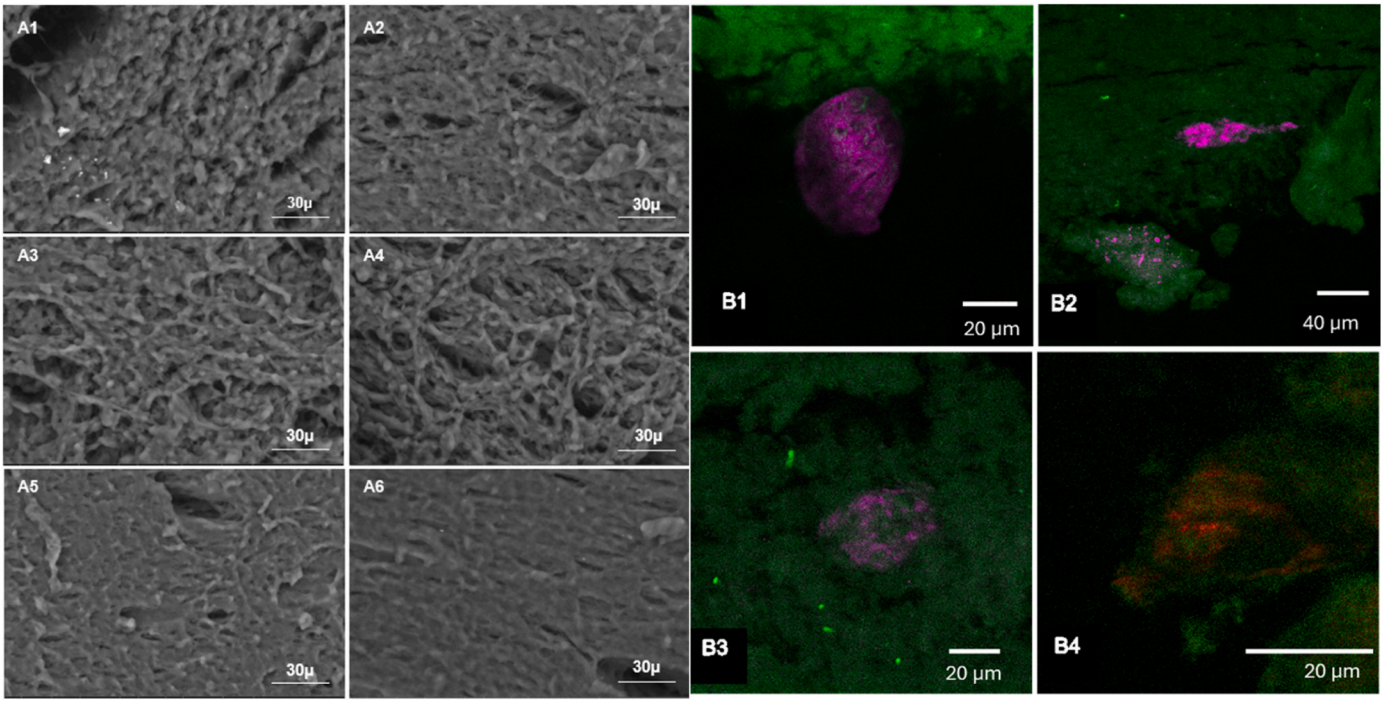

Fig. 7. (A) *Scanning electron micrographs of extruded composite pea protein-cultured meat cell samples. Micrographs are viewed at magnification in the range 1987-2468x along the axis of extrusion (A1 (2415 x), A3 (2363x) and A5 (1987x)) and perpendicular to the axis of extrusion (A2 (2468x), A4 (2312x) and A6 (2312x)). Micrographs A1, and A2 are for control samples with no added meat cells; A3 and A4 have 2 % added cells; A5 and A6 have 10 % added meat cells.* (B) *Confocal micrographs of the extruded sample containing 10 % of cells. Nuclear material (nuclei and/or DNA) are stained with Hoechst 33342 and represented in false colour as magenta, actin is stained with phalloidin- ATTO752 and is represented in red, and the auto fluorescence of the protein network is represented in green.* (For interpretation of the references to colour in this figure legend, the reader is referred to the Web version of this article.)

The nonlinear rheological fingerprints observed in LAOS (Fig. 6) strongly correlate with textural properties and underlying protein–protein interactions. *E*-PCB10 exhibiting delayed onset of nonlinearity, pronounced elastic strain stiffening, and reduced viscous dissipation has typically formed more cohesive, load-bearing networks than *E*-PCB2, which align with higher hardness, elasticity, and water retention reported (Klost & Drusch, 2019; Moakes et al., 2015). These behaviours reflect microstructural integrity under large deformation, where compatibility or semi-compatibility between proteins promotes integrated gel networks rather than phase-separated domains (Lin & Barbut, 2024; Shen et al., 2022; Sun & Arntfield, 2012). In contrast, *E*-PPI and *E*-PCB2 with early yielding and weak elastic loops often correspond to incompatibility, resulted in heterogeneous structures and diminished mechanical strength. Recent studies applying LAOS to high moisture extrudates confirm its utility in diagnosing structural anisotropy and network robustness under large deformation, linking nonlinear viscoelasticity to fibrous texture development and protein alignment during extrusion (Sui et al., 2024; D. Sun et al., 2022; Y. Zhang, Zhao, et al., 2022a). Thus, LAOS provides a mechanistic link between nonlinear viscoelasticity, textural performance, and protein interaction type in hybrid alternative protein extrudates, complementing frequency sweep data and compositional analysis (Ewoldt & McKinley, 2010; Hyun et al., 2011; Y. Wang & Selomulya, 2022c). Comparable structure-function coupling has been reported for heat-modulated pea protein composites (Bhuiyan et al., 2025) as well as protein–hydrocolloid matrices offering water retention in meat analogues, complementing extrusion-built networks (Bhuiyan et al., 2024a).

3.4. Influence of microstructural change

Scanning electron micrographs of pea protein extrudate *E*-PPI, and hybrid pea protein extrudate samples *E*-PCB2 and *E*-PCB10 respectively are shown in Fig. 7 as well as Figs. S2 and S3 in the Supplementary information. Two different views, one that looks along and another perpendicular to the axis of extrusion, are presented. At a magnification of 100x, the lamination in the control sample *E*-PPI looking down the extrusion axis is clearly visible as concentric elliptical layers of protein (Fig. S3a in Supplementary information). The lamination is also visible in EPCB2 (Fig. S2c in Supplementary information) and *E*-PCB10 (Fig. S2e in Supplementary information), although the presence of elliptical shells is less apparent, and larger vacancies appear between the layers. The features of the lamination change as more CB are added, and larger vacancies are formed with increasing concentration of CB. One might expect the samples to undergo extensional shear as they are extruded through the cool die, and for linear layers to be seen in the SEM micrographs viewed perpendicular to the extrusion axis. Whilst distinct layers are visible (Figs. S2b, S2d, and S2f in Supplementary information), somewhat surprisingly these are non-linear. For the samples containing cells (Fig. S2c–S2f in Supplementary information) there were no obvious cell-like structures visible at both concentrations.

Increasing the magnification to between 854-972x reveals further ultrastructure (Fig. S3 in Supplementary information). The control sample *E*-PPI shows evidence of discrete protein fibrils (Fig. S3a in Supplementary information) that aggregate to form the gelled microstructure, although these are less obvious when viewed perpendicular to the direction of extrusion (Fig. S3b in Supplementary information). After addition of 2 % w/w of CB, the fibril-like aggregates are more pronounced in *E*-PCB2 and are visible both in the direction of extrusion (Fig. S3c in Supplementary information) and perpendicular to this (Fig. S3d in Supplementary information). When the CB concentration is increased to 10 %, the protein fibrils in *E*-PCB10 largely disappear (Fig. S3e and S3f in Supplementary information). A further increase in magnification to between 1987-2468x (Fig. 7) supports Fig. S2 in that fibril-like structures can be seen in the control samples E-PPI (Fig. 7 A1-2), becoming more pronounced in E-PCB2 (Fig. 7 A3, A4), but largely disappear in *E*-PCB10 (Fig. 7 A5, A6). This CB-dependent shift from

pronounced fibrillation (2 %) toward a less fibrillar network (10 %) mirrors reports that tuning plant-protein composite ratios can switch networks between fibrous/porous morphologies and thereby impact consumer acceptance (Bhuiyan et al., 2024b).

There are no obvious cultivated meat cells visible in any of the SEM micrographs, even at the highest magnification. A selection of confocal microscopy imaging revealed only a few structures that could be cell nuclear material or actin filaments and only in *E*-PCB10 (Fig. 7B). The microstructures analysis using confocal microscopy via staining with Hoescht 33342 showed no stained features in the micrographs (Fig. 7 B1-B3) with correct dimensions for cell nuclei (typically 5–10 μm). This suggests that these may be CB where the nucleus has been disrupted, and DNA released. Similarly, we only see one structure (Fig. 7 B4) that stains with phalloidin- ATTO752, and this is rather diffuse and indistinct. Taken together, the SEM and confocal microscopy suggest that the added cells are largely disrupted during HME and few, if any remain intact after processing.

The SEM and confocal results suggest compatibility or semi-compatibility between pea protein and CB components, as evidenced by altered fibril morphology and network integration rather than distinct phase separation. This interpretation is consistent with observed improvements in texture and water retention in hybrid systems (Lin & Barbut, 2024; Shen et al., 2022; Sun & Arntfield, 2012; Zhu et al., 2022).

3.5. Off-flavour reduction and taste modulation

Legume proteins including pea are known to have beany off-flavour (Mittermeier-Kleßinger et al., 2021), bitterness and astringency (Karolkowski et al., 2023; Lesme et al., 2024; Xia et al., 2022). Key volatile marker compounds previously reported for the beany off-flavour of pea protein were analysed for *E*-PPI, *E*-PCB2 and *E*-PCB10: 2-pentylfuran, 2,4-decadienal and hexanal (Supplementary Fig. S1) (Xiang et al., 2023). The importance of flavour including masking typical off-odourants of plant protein had been highlighted in several studies in determining consumer acceptance of plant-based meat analogues (Cordelle et al., 2022; Y. Wang, Kadyan, et al., 2022).

The release of both hexanal and 2,4-decadienal increases in hybrid extrudate *E*-PCB2 compared to faba protein only extrudate *E*-PPI (Fig. 8 A2, A3). However, the intensity of all three key markers for beany off-flavour is lowest in *E*-PCB10 when compared to *E*-PPI (Fig. 8A) which indicates decreasing level of beany off-flavour in hybrid pea protein extrudates with increasing addition of CB.

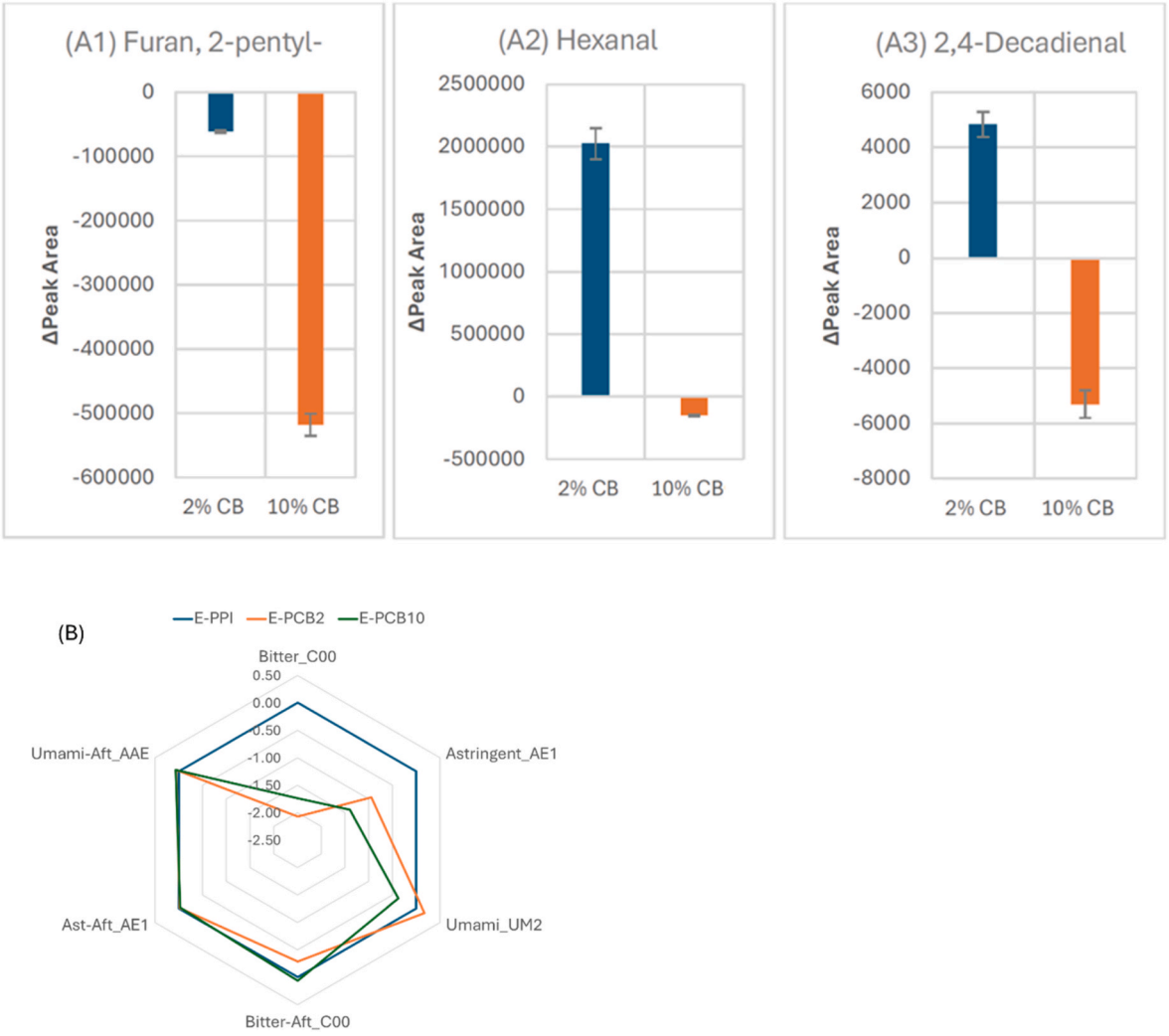

Fig. 8. (A) *The key off-odourants were analysed using Centri-GC×GC-TOFMS (see materials and method for details). The relative amounts (equivalent to the pea area difference, Δ Peak Area) of 2-Pentyl furan (Panel A1), hexanal (Panel A2) and 2,4-Decadienal (Panel A3) due to addition of 2 % and 10 % CB to the pea protein in HME were estimated* using equation (1a) *(effect of 2 % CB = Δ2 %CB, Δ Peak Area = peak area of E-PCB2 – peak area of E-PPI) and 1b (effect of 10 % CB = Δ10 %CB, Δ Peak Area = peak area of E-PCB10 – peak area of E-PPI) as described under section experimental design. The negative value of Δ Peak Area illustrates lower release of volatiles compared to E-PPI whereas positive value depicts higher release.* (B) *Taste analysis of extrudates made of only pea protein isolate (E-PPI), and that of pea protein isolate mixed with 2 % and 10 % w/w CB, E-PCB2 and E-PCB10 respectively.*

For visualization of taste differences as illustrated in Fig. 8B, a relative comparison of the off-taste like bitterness and astringency including the after taste as well as umami profile of *E*-PCB2 and *E*-PCB10 was performed by taking *E*-PPI as control. *E*-PCB10 exhibited significantly lower astringency compared to the control. Both hybrid pea protein extrudates possess reduced bitterness compared to *E*-PPI, but there was no perceivable difference in bitterness between *E*-PCB2 and EPCB10 (Fig. 8B).

3.6. Multivariate analysis and PCA-based clustering to explore functional relationships in hybrid extrudates

As HME process parameters remained constant for *E*-PPI, *E*-PCB2 and *E*-PCB10, the difference in texture and other structural and functional attributes should be related to molecular properties of PPI and CB. This study unequivocally demonstrates that a 10 % incorporation of CB into pea protein under HME significantly modulates the texture quality, water and oil holding capacities, and sensory properties. *E*-PCB10 is associated with lower SME and a change in microstructure from an elongated fibrous, porous, open structure in *E*-PPI and *E*-PCB2 to a denser, cohesive protein network structure where the elongated fibrils are largely absent. The disruption of pea protein matrix by 10 % w/w of cultivated beef upon HME appears to create new interaction networks that enhance the overall structural integrity of *E*-PCB10. This is supported by highest inter-molecular disulphide bond induced cross-linking in *E*-PCB10 (Fig. 4) as well as LAOS study on extrudates (Fig. 6) which manifesting cohesive network and higher mechanical strength of *E*-PCB10. The denser microstructure of the *E*-PCB10 as observed in SEM analysis clearly leads to enhanced mechanical properties as demonstrated by higher toughness, firmness and extensibility along with increased ability to retain water and oil compared to *E*-PCB2. This is also supported by enhanced protein cross-linking via inter-molecular disulfide bonds between PPI and CB observed in *E*-PCB10 (Fig. 4) enabling higher fibrous structure. Such relationship of decreasing SME with concomitant microstructural change upon HME showing a stronger gel network in *E*-PCB10 is consistent with protein interaction studies of extrudates (Fig. 4) as well as reported in other studies on hybrid meat products (Alam et al., 2024; Kim et al., 2024; Santos et al., 2022).

In order to better understand the variables influencing the differentiation among extrudates, 27 determined parameters as variables; *E*-PPI, *E*-PCB2 and *E*-PCB10 as observations were introduced into Principal Component Analysis (PCA) and a Hierarchical Cluster Analysis (HCA) for better clustering visualization. Two distinct clusters were formed along PC1, as shown in Fig. 9A, with *E*-PPI and *E*-PCB2 on one side and *E*-PCB10 on the other. The same clustering pattern was also visualized in the HCA plot in Fig. S1B in Supplementary information.

According to the score contribution analysis (Fig. S1 in Supplementary information), the variables WHC, extensibility, degree of texturization (DT), OHC, resistance to extension, adhesiveness, 2-pentylfuran, and springiness were identified as important parameters in differentiating *E*-PCB10. According to ANOVA analysis, WHC, extensibility, OHC, resistance to extension and adhesiveness are significantly higher in *E*-PCB10 compared to *E*-PCB2 (Figs. 1 and 5). These differences are due to the microstructural transformation of the pea protein matrix upon HME induced by the incorporation of 10 % CB. As observed in the microstructure analysis, increased CB disrupts further the native laminar structure of PPI upon HME, promoting the formation of a denser, more cohesive protein network in *E*-PCB10. Such denser matrix enhances mechanical properties such as hardness, extensibility, and adhesiveness (Fig. 5A), while also improving oil and water retention (Fig. 1A and B). The lower SME suggests a more viscoelastic melt during extrusion, potentially due to the plasticizing effect of intracellular components released from disrupted CBs (Schmid et al., 2022). The reduction in springiness in pea protein extrudate with 10 % CB (Fig. 5A) may reflect a more compact and less elastic protein network due to significantly high cross-linking via intermolecular S-S bonding in *E*-PCB10 as shown in Fig. 4. A similar change in springiness was observed in a study of hybrid meat (Kim et al., 2024). These findings therefore support the hypothesis that hybrid formulations with cultivated meat cells can significantly enhance both the functional and flavour properties as well as reduce off-odourant of pea protein-based meat analogues.

To elucidate the pairwise relationships between variables,

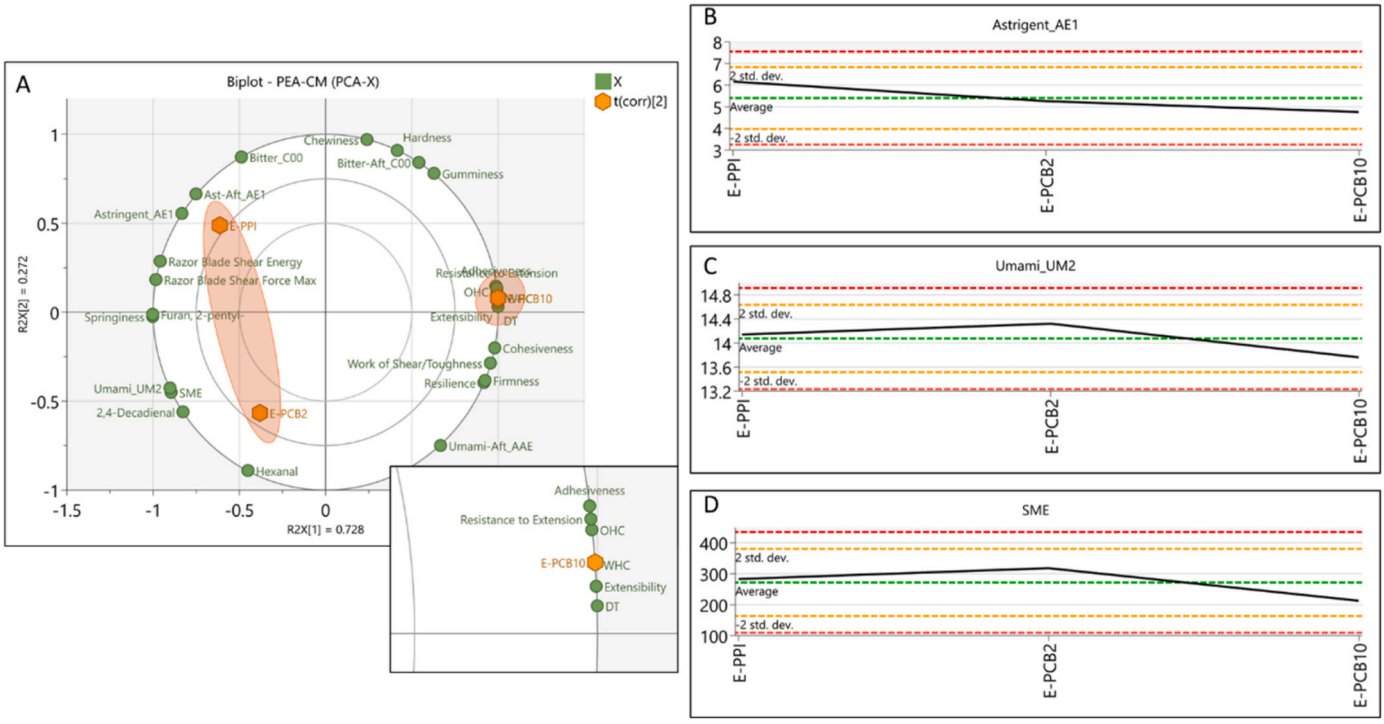

Fig. 9. *(A) PCA Biplot to reveal the relationship between the taste, flavour and texture, E-PCB10 is distinguished from E-PPI and E-PCB2. Panels (B), (C), and (D) illustrate the changes in astringency, umami, and SME with increasing %CB.*

particularly off-odourants and taste versus texture, a correlation matrix was performed (Table S4 in Supplementary information). A strong positive linear correlation (coefficient >0.8) was observed between 3 off-odourants and SME, indicating that the extrusion process influences the release of aroma compounds.

Hexanal belongs to the aldehyde group, which is known for its strong binding affinity to proteins (Y. Wang, Kadyan, et al., 2022) however, hexanal has a low molecular weight and among the three off-odourants markers, it exhibited the smallest relative decrease in *E*-PCB10 (Fig. 8A). Examining the correlation between the three off-odourants and additional texture parameters may explain this. The correlation coefficients between cohesiveness and 2-pentylfuran; 2,4-decadienal were −0.98 and −0.70 (Table S4 in Supplementary information), respectively, whereas the correlation with hexanal was only −0.26. A similar trend was observed with adhesiveness, a parameter indicative of texture smoothness: the correlation coefficients were −0.99 and −0.90 for 2-pentylfuran, and 2,4-decadienal, respectively, while hexanal showed a weaker correlation of −0.58 (Table S4 in Supplementary information).

This may be attributed to hexanal's low molecular weight and high volatility, which likely made the inhibition of its release less susceptible than the other off-odourants to the more adhesive-like texture change in *E*-PCB10. Similar findings were reported in a study investigating how hydrocolloid thickeners altered the release of low-molecular-weight aroma volatiles (Cook et al., 2005).

Interestingly, while hexanal exhibited a relatively low release in *E*-PCB10, it demonstrated the highest release in *E*-PCB2, increasing by 207.9 % compared to *E*-PPI. This disparity may be attributed to the more porous texture observed in *E*-PCB2 compared to *E*-PPI and *E*-PCB10 (Figure S3 (a, c, e) in Supplementary information). The enhanced porosity likely facilitates the migration of low-molecular-weight volatile compounds, contributing to the increased release of hexanal in *E*-PCB2. Additionally, hexanal showed a strong negative correlation with hardness ($r < -0.99$), reinforcing the matrix effect in terms of the relationship between porous matrix structure and volatile compound release.

Astringency, primarily attributed to tannins in peas, significantly affects consumer acceptance of plant-based products, particularly meat analogues (Lesme et al., 2024). The addition of CB notably reduces astringency, with EPCB-10 exhibiting the lowest levels (Fig. 9B). Similarly, bitterness, likely derived from medium to high molecular weight saponins in peas (Xia et al., 2022), is noticeably mitigated by a 2 % CB addition compared to the extrudate with only pea protein, *E*-PPI. These findings clearly suggest that presence of CB inhibit the release of middle to high molecular weight tannins and saponins, reducing off-taste of plant protein extrudates.

Umami, a desirable characteristic in meat analogues, is influenced by both CB addition and the presence of monosodium glutamate (MSG) in pea protein isolate (Ongkowijoyo & Peterson, 2023). Unlike astringency and bitterness attributing compounds, which have moderate to high molecular weights, MSG (169.1 Da) exhibits a strong positive linear correlation with SME (coefficient >0.99, Table S4 in Supplementary information). Fig. 9C and D illustrate a correlation between lower SME and reduced umami intensity which implies that a stronger gel network in *E*-PCB10 may limit umami compound release. However, such inhibition is minimal, with a unit change <1 when compared *E*-PCB10 to *E*-PPI which corroborates with their observed changes in SME and microstructure. While the correlation analysis was based on limited three sample levels, the observed trends provide valuable initial insights into the interactions between off-odourants, taste compounds and texture parameters. Additionally, it is important to note that the correlations observed do not imply causation, rather, they highlight potential associations that suggest expanding the study to include a broader range of sample levels in future work could help to further validate and deepen understanding these findings.

4. Conclusions

This work highlights a transformative advance in hybrid alternative protein approach by leveraging co-extrusion of pea protein with cultivated beef. The minimal quantity of cultivated beef has significantly modulated the texture, physicochemical and taste and aroma properties of the pea protein extrudate which prompted an enhancement of functional properties of hybrid alternative protein. This study has unequivocally demonstrated that co-extrusion of hybrid alternative protein mixtures involves a complex interplay between the extent of denaturation, surface hydrophobicity, consolidation of newly formed protein-protein networks, and the development of fibril morphology which is dependent on level of cultivated meat incorporation. Overall, the results clearly highlight the opportunity for high moisture extrusion-based texture modulation and microstructural transformation of plant protein by mixing with other source of alternative protein. Such successful integration of cultivated beef with pea protein isolate has manifested, for the first time, a unique texturization opportunity via microstructure modulation using high moisture extrusion to generate hybrid alternative protein extrudate. This study also showed the effectiveness of minimal quantities of cultivated beef, hitherto not reported, to improve the taste and flavour properties of textured pea protein by lowering the release of key molecules of pea protein known for imparting off flavour.

The HME process has strengthened the PPI-CB protein network in *E*-PCB10 relative to *E*-PCB2 through enhanced cross-linking via intermolecular disulfide bond formation along with other hydrophobic interactions. This strengthening via cross-linking was attributed to the increased CB availability in *E*-PCB10, which concurrently altered the fibril morphology compared to *E*-PCB2. The SEM imaging demonstrated these morphological changes, while LAOS analysis confirmed the improved structural resilience of *E*-PCB10.

This breakthrough study exhibits that co-extrusion using hybrid mix of alternative protein formulation can overcome the individual limitations of both plant-based and cultivated meat technologies while capitalizing on their respective strengths. Besides, it also addresses one of the present challenges of cultivated meat sector – the production scale and cost, by demonstrating that cultivated beef can rather act as high impact functional ingredient in plant-based meat. Different alternative protein sources demonstrate varying response to thermos-mechanical process and therefore integrating multiple protein sources in HME process requires further understanding of individual protein behaviour in presence of one another. As the relationship between feed types, process parameters and product qualities are known to be non-linear, our future research will focus on optimizing co-extrusion parameters to maximize the synergistic effects between cultivated meat cells and various other plant proteins to achieve best possible functional, nutritional and sensory properties.

CRediT authorship contribution statement

Vahid Baeghbali: Writing – review & editing, Writing – original draft, Visualization, Validation, Investigation, Formal analysis, Data curation. **Stephen R. Euston:** Writing – review & editing, Writing – original draft, Investigation, Formal analysis, Data curation. **Xi He:** Writing – review & editing, Writing – original draft, Visualization, Investigation, Formal analysis, Data curation. **Manuela Donetti:** Writing – review & editing, Resources. **Osama Maklad:** Data curation, Formal analysis, Investigation, Visualization, Writing – review & editing. **Parag Acharya:** Writing – review & editing, Writing – original draft, Visualization, Supervision, Funding acquisition, Conceptualization.

Ethics declaration

This study does not involve any animal or human subjects.

Declaration of competing interest

The authors declare that they have no known competing financial interests or personal relationships that could have appeared to influence the work reported in this paper.

Acknowledgements

P.A. acknowledges funding from Bezos Earth Fund through the Bezos Centre for Sustainable Protein (BCSP/IC/001) and financial support from the UK Government funding provided through UK Research and Innovation's flagship Strength in Places grant. We thank Dr Jim Buckman of the Centre for Environmental Scanning Electron Microscopy (CESEM), HWU and Dr Jessica Vali, Edinburgh Super-Resolution Imaging Consortium (ESRIC), HWU for SEM and CLSM imaging respectively.

Appendix A. Supplementary data

Supplementary data to this article can be found online at https://doi.org/10.1016/j.foodhyd.2025.112154.

Data availability

The raw experimental data and derived results that support the findings of the study are provided in the main text and Supplementary Information. Any additional data will be made available on request. The experimental methodologies used in this study are described and referenced under section Materials and Methods.

References

Abdul Kareem, F. B., Nicholles, B., & Bryant, C. (2024). Consumer acceptance of alternative proteins: A Re-Review. *Food Reviews International*, 1–22. https://doi.org/10.1080/87559129.2024.2405051

Alam, A. N., Kim, C.-J., Kim, S.-H., Kumari, S., Lee, S.-Y., Hwang, Y.-H., & Joo, S.-T. (2024). Trends in hybrid cultured meat manufacturing technology to improve sensory characteristics. *Food Science of Animal Resources, 44*(1), 39–50. https://doi.org/10.5851/kosfa.2023.e76

An, J.-H., & Kim, H.-Y. (2024). Scaffolds bioink for 3D bioprinting. *Food Science of Animal Resources*. https://doi.org/10.5851/kosfa.2024.e120

Anusha Siddiqui, S., Bahmid, N. A., Mahmud, C. M. M., Boukid, F., Lamri, M., & Gagaoua, M. (2023). Consumer acceptability of plant-, seaweed-, and insect-based foods as alternatives to meat: A critical compilation of a decade of research. *Critical Reviews in Food Science and Nutrition, 63*(23), 6630–6651. https://doi.org/10.1080/10408398.2022.2036096

Arora, S., Kataria, P., Nautiyal, M., Tuteja, I., Sharma, V., Ahmad, F., Haque, S., Shahwan, M., Capanoglu, E., Vashishth, R., & Gupta, A. K. (2023). Comprehensive review on the role of plant protein as a possible meat analogue: Framing the future of meat. *ACS Omega, 8*(26), 23305–23319. https://doi.org/10.1021/acsomega.3c01373

Badii, F., Atri, H., & Dunstan, D. E. (2016). The effect of shear on the rheology and structure of heat-induced whey protein gels. *International Journal of Food Science and Technology, 51*(7), 1570–1577. https://doi.org/10.1111/ijfs.13126

Baig, M. A., Ajayi, F. F., Hamdi, M., Baba, W., Brishti, F. H., Khalid, N., Zhou, W., & Maqsood, S. (2024). Recent research advances in meat analogues: A comprehensive review on production, protein sources, quality attributes, analytical techniques used, and consumer perception. *Food Reviews International*, 1–32. https://doi.org/10.1080/87559129.2024.2396855

Barnés-Calle, C., Matas, G., Claret, A., Guerrero, L., Fulladosa, E., & Gou, P. (2024). High moisture extrusion of pea protein isolate to mimic chicken texture: Instrumental and sensory insights. *Food Hydrocolloids, 154*, Article 110129. https://doi.org/10.1016/j.foodhyd.2024.110129

Bhuiyan, M. H. R., Liu, L., Samaranayaka, A., & Ngadi, M. (2025). Characterization of pea composites and feasibility of heat-modulated meat analogs production. *Food Chemistry, 463*, Article 141282. https://doi.org/10.1016/j.foodchem.2024.141282

Bhuiyan, M. H. R., Yeasmen, N., & Ngadi, M. (2024a). Impact of hydrocolloids on 3D meat analog printing and cooking. *Food Structure, 42*, Article 100396. https://doi.org/10.1016/j.foostr.2024.100396

Bhuiyan, M. H. R., Yeasmen, N., & Ngadi, M. (2024b). Restructuring plant-derived composites towards the production of meat-analog based coated fried food. *Food Chemistry, 443*, Article 138482. https://doi.org/10.1016/j.foodchem.2024.138482

Bomkamp, C., Skaalure, S. C., Fernando, G. F., Ben-Arye, T., Swartz, E. W., & Specht, E. A. (2022). Scaffolding biomaterials for 3D cultivated meat: Prospects and challenges. *Advanced Science, 9*(3). https://doi.org/10.1002/advs.202102908

Cheng, E. M. Y., Cheng, C. M. L., Choo, J., Yan, Y., & Carrasco, L. R. (2024). Biodiversity footprints of 151 popular dishes from around the world. *PLoS One, 19*(2), Article e0296492. https://doi.org/10.1371/journal.pone.0296492

Clark, M. A., Domingo, N. G. G., Colgan, K., Thakrar, S. K., Tilman, D., Lynch, J., Azevedo, I. L., & Hill, J. D. (2020). Global food system emissions could preclude achieving the 1.5° and 2°C climate change targets. *Science, 370*(6517), 705–708. https://doi.org/10.1126/science.aba7357

Cook, D. J., Hollowood, T. A., Linforth, R. S. T., & Taylor, A. J. (2005). Correlating instrumental measurements of texture and flavour release with human perception. *International Journal of Food Science and Technology, 40*(6), 631–641. https://doi.org/10.1111/J.1365-2621.2005.00973.X

Cordelle, S., Redl, A., & Schlich, P. (2022). Sensory acceptability of new plant protein meat substitutes. *Food Quality and Preference, 98*, Article 104508. https://doi.org/10.1016/J.FOODQUAL.2021.104508

Dahl, J. F., Bouché, O., Schlangen, M., der Goot, A. J. van, & Corredig, M. (2025). Relationship between rheological parameters and structure formation in high moisture extrusion of plant protein biopolymers. *Food Hydrocolloids, 160*, Article 110843. https://doi.org/10.1016/j.foodhyd.2024.110843

De Angelis, D., van der Goot, A. J., Pasqualone, A., & Summo, C. (2024). Advancements in texturization processes for the development of plant-based meat analogs: A review. *Current Opinion in Food Science, 58*, Article 101192. https://doi.org/10.1016/j.cofs.2024.101192

Deliza, R., Rodríguez, B., Reinoso-Carvalho, F., & Lucchese-Cheung, T. (2023). Cultured meat: A review on accepting challenges and upcoming possibilities. *Current Opinion in Food Science, 52*, Article 101050. https://doi.org/10.1016/j.cofs.2023.101050

Deloitte, L. L. A. (2019). *Plant-based alternatives driving industry M&A*.

Dreoni, I., Matthews, Z., & Schaafsma, M. (2022). The impacts of soy production on multi-dimensional well-being and ecosystem services: A systematic review. *Journal of Cleaner Production, 335*, Article 130182. https://doi.org/10.1016/j.jclepro.2021.130182

Erturk, M. Y., Le, A. N. M., & Kokini, J. (2023). Advances in large amplitude oscillatory shear rheology of food materials. *Frontiers in Food Science and Technology, 3*. https://doi.org/10.3389/frfst.2023.1130165

Ewoldt, R. H., & McKinley, G. H. (2010). On secondary loops in LAOS via self-intersection of lissajous–bowditch curves. *Rheologica Acta, 49*(2), 213–219. https://doi.org/10.1007/s00397-009-0408-2

Feng, Z., He, D., Zhang, L., Li, Q., Xue, C., Yi, X., Liao, L., Pei, Z., & Shen, X. (2025). Preparation of myofibrillar protein oleogels by emulsion template method: Application of fat substitute for sponge cakes. *Lebensmittel-Wissenschaft & Technologie.* , Article 117350. https://doi.org/10.1016/j.lwt.2025.117350

Ferawati, F., Zahari, I., Barman, M., Hefni, M., Ahlström, C., Witthöft, C., & Östbring, K. (2021). High-moisture meat analogues produced from yellow pea and faba bean protein isolates/concentrate: Effect of raw material composition and extrusion parameters on texture properties. *Foods, 10*(4), 843. https://doi.org/10.3390/foods10040843

Flory, J., Xiao, R., Li, Y., Dogan, H., Talavera, M. J., & Alavi, S. (2023). Understanding protein functionality and its impact on quality of plant-based meat analogues. *Foods, 12*(17), 3232. https://doi.org/10.3390/foods12173232

Gaber, S. M., Knezevic, D., Saldanha do Carmo, C., Zobel, H., Knutsen, S. H., Sahlstrøm, S., & Dessev, T. (2023). Meat analogues from pea protein: Effect of different oat protein concentrates and post treatment on selected technological properties of high-moisture extrudates. *Applied Sciences, 13*(22), Article 12354. https://doi.org/10.3390/app132212354

Garrison, G. L., Biermacher, J. T., & Brorsen, B. W. (2022). How much will large-scale production of cell-cultured meat cost? *Journal of Agriculture and Food Research, 10*, Article 100358. https://doi.org/10.1016/j.jafr.2022.100358

Huamaní-Perales, C., Vidaurre-Ruiz, J., Salas-Valerio, W., Cabezas, D. M., & Repo-Carrasco-Valencia, R. (2024). A review of techno-functional properties of legume proteins and their potential for development of new products. *European Food Research and Technology 2024, 250*(8), 2069–2092. https://doi.org/10.1007/S00217-024-04536-6, 250:8.

Hubalek, S., Post, M. J., & Moutsatsou, P. (2022). Towards resource-efficient and cost-efficient cultured meat. *Current Opinion in Food Science, 47*, Article 100885. https://doi.org/10.1016/j.cofs.2022.100885

Humpenöder, F., Bodirsky, B. L., Weindl, I., Lotze-Campen, H., Linder, T., & Popp, A. (2022). Projected environmental benefits of replacing beef with microbial protein. *Nature, 605*(7908), 90–96. https://doi.org/10.1038/s41586-022-04629-w

Hyun, K., Wilhelm, M., Klein, C. O., Cho, K. S., Nam, J. G., Ahn, K. H., Lee, S. J., Ewoldt, R. H., & McKinley, G. H. (2011). A review of nonlinear oscillatory shear tests: Analysis and application of large amplitude oscillatory shear (LAOS). *Progress in Polymer Science, 36*(12), 1697–1753. https://doi.org/10.1016/j.progpolymsci.2011.02.002

Jang, J., & Lee, D.-W. (2024). Advancements in plant based meat analogs enhancing sensory and nutritional attributes. *Npj Science of Food, 8*(1), 50. https://doi.org/10.1038/s41538-024-00292-9

Jareonsin, S., Pumas, C., Jaitiang, D., & Uttarota, T. (2024). Green fusion proteins: An approach to sustainable nutrition blending plant and algae-based proteins for a circular food system. *Future Foods, 10*, Article 100415.

Jiang, W., Feng, J., Yang, X., & Li, L. (2024). Structure of pea protein-based complexes on high-moisture extrusion: Raw materials and extrusion zones. *Lebensmittel-Wissenschaft & Technologie, 194*, Article 115823. https://doi.org/10.1016/j.lwt.2024.115823

Jiménez-Munoz, L. M., Tavares, G. M., & Corredig, M. (2021). Design future foods using plant protein blends for best nutritional and technological functionality. *Trends in Food Science & Technology, 113*, 139–150. https://doi.org/10.1016/J.TIFS.2021.04.049

Kaplan, D. L., & McClements, D. J. (2025). Hybrid alternative protein-based foods: Designing a healthier and more sustainable food supply. *Frontiers in Science, 3*. https://doi.org/10.3389/fsci.2025.1599300

Karolkowski, A., Belloir, C., Briand, L., & Salles, C. (2023). Non-volatile compounds involved in bitterness and astringency of pulses: A review. *Molecules, 28*(8), 3298. https://doi.org/10.3390/molecules28083298

Kim, S.-H., Kumari, S., Kim, C.-J., Lee, E.-Y., Alam, A. N., Chung, Y.-S., Hwang, Y.-H., & Joo, S.-T. (2024). Effect of adding cultured meat tissue on physicochemical and taste characteristics of hybrid cultured meat manufactured using wet-spinning. *Food Science of Animal Resources, 44*(6), 1440–1452. https://doi.org/10.5851/kosfa.2024.e104

Klost, M., & Drusch, S. (2019). Structure formation and rheological properties of pea protein-based gels. *Food Hydrocolloids, 94*, 622–630. https://doi.org/10.1016/j.foodhyd.2019.03.030

Lampinen, J., Harinen, R., Perälä, A., & Raitio, M. (2014). Determination of protein unfolding using UV-fluorometry. In *Application note poster*. Thermo Fisher Scientific. https://documents.thermofisher.com/TFS-Assets/LCD/posters/Poster-SLAS-2014-Determination-of-Protein-Unfolding-Using-UV-fluorometry.pdf.

AOAC official method 2008.06Moisture and fat in meats. In Latimer, G. W. (Ed.), *Official methods of analysis of AOAC INTERNATIONAL*, (2023). Oxford University Press. https://doi.org/10.1093/9780197610145.003.3469.

Lee, J., Kim, S., Jeong, Y. J., Choi, I., & Han, J. (2023a). Impact of interactions between soy and pea proteins on quality characteristics of high-moisture meat analogues prepared via extrusion cooking process. *Food Hydrocolloids, 139*, Article 108567. https://doi.org/10.1016/j.foodhyd.2023.108567

Lee, S. Y., Lee, D. Y., Jeong, J. W., Kim, J. H., Yun, S. H., Joo, S.-T., Choi, I., Choi, J. S., Kim, G.-D., & Hur, S. J. (2023b). Studies on meat alternatives with a focus on structuring technologies. *Food and Bioprocess Technology, 16*(7), 1389–1412. https://doi.org/10.1007/s11947-022-02992-0

Leffler, T. P., Moser, C. R., McManus, B. J., Urh, J. J., Keeton, J. T., Claflin, A., Adkins, K., Claflin, A., Davis, C., Elliot, J., Goin, P., Horn, C., Humphries, J., Ketteler, K., Perez, P., & Steiner, G. (2008). Determination of moisture and fat in meats by microwave and nuclear magnetic resonance analysis: Collaborative study. *Journal of AOAC International, 91*(4), 802–810. https://doi.org/10.1093/jaoac/91.4.802

Lesme, H., Kew, B., Bonnet, L., Sarkar, A., & Stellacci, F. (2024). Difference in astringency of the main pea protein fractions. *Food Hydrocolloids, 149*, Article 109489. https://doi.org/10.1016/J.FOODHYD.2023.109489

Li, J., & Li, L. (2023). Effect of extrusion temperature on the structure and emulsifying properties of soy protein isolate-oat β-glucan conjugates formed during high moisture extrusion. *Food Chemistry, 429*, Article 136787. https://doi.org/10.1016/j.foodchem.2023.136787

Lin, W., & Barbut, S. (2024). Hybrid meat batter system: Effects of plant proteins (pea, brown rice, faba bean) and concentrations (3–12%) on texture, microstructure, rheology, water binding, and color. *Poultry Science, 103*(7), Article 103822. https://doi.org/10.1016/j.psj.2024.103822

Lindberg, L., McCann, R. R., Smyth, B., Woodside, J. V., & Nugent, A. P. (2024). The environmental impact, ingredient composition, nutritional and health impact of meat alternatives: A systematic review. *Trends in Food Science & Technology, 149*, Article 104483. https://doi.org/10.1016/j.tifs.2024.104483

Liu, X., Zhao, Y., Li, K., Shen, S., & Li, J. (2024). Exploring the mechanism of amylose/amylopectin improving formation of yeast-soy protein high-moisture extrudates based on small and large amplitude oscillatory shear rheology. *Food Hydrocolloids, 153*, Article 110062. https://doi.org/10.1016/j.foodhyd.2024.110062

Lurie-Luke, E. (2024). Alternative protein sources: Science powered startups to fuel food innovation. *Nature Communications, 15*(1), 4425. https://doi.org/10.1038/s41467-024-47091-0

Malila, Y., Owolabi, I. O., Chotanaphuti, T., Sakdibhornssup, N., Elliott, C. T., Visessanguan, W., Karoonuthaisiri, N., & Petchkongkaew, A. (2024). Current challenges of alternative proteins as future foods. *Npj Science of Food, 8*(1), 53. https://doi.org/10.1038/s41538-024-00291-w

Mittermeier-Kleßinger, V. K., Hofmann, T., & Dawid, C. (2021). Mitigating off-flavors of plant-based proteins. *Journal of Agricultural and Food Chemistry, 69*(32), 9202–9207. https://doi.org/10.1021/acs.jafc.1c03398

Moakes, R. J. A., Sullo, A., & Norton, I. T. (2015). Preparation and rheological properties of whey protein emulsion fluid gels. *RSC Advances, 5*(75), 60786–60795. https://doi.org/10.1039/C5RA12684C

Muhialdin, B. J., Flores Sanchez, C., Nakagawa, H., & Ubbink, J. (2024). Modulating molecular interactions in extruded pea protein isolate. *Food Biophysics, 19*(1), 172–181. https://doi.org/10.1007/s11483-023-09813-7

Munialo, C. D. (2024). A review of alternative plant protein sources, their extraction, functional characterisation, application, nutritional value and pinch points to being the solution to sustainable food production. *International Journal of Food Science and Technology, 59*(1), 462–472. https://doi.org/10.1111/ijfs.16467

Ongkowijoyo, P., & Peterson, D. G. (2023). Identification of compounds contributing to umami taste of pea protein isolate. *Food Chemistry, 429*, Article 136863. https://doi.org/10.1016/J.FOODCHEM.2023.136863

Osen, R., Toelstede, S., Eisner, P., & Schweiggert-Weisz, U. (2015). Effect of high moisture extrusion cooking on protein–protein interactions of pea (*pisum sativum* L.) protein isolates. *International Journal of Food Science and Technology, 50*(6), 1390–1396. https://doi.org/10.1111/ijfs.12783

Oxford University Environmental Change Institute. (2021). *Resilience of the UK food system regarding demand for soy. Policy and practice brief*. Food system resilience programme. https://www.eci.ox.ac.uk/sites/default/files/2022-07/FSR-soy-demand-chains_NOV21.pdf.

Ozturk, O. K., & Hamaker, B. R. (2023). Texturization of plant protein-based meat alternatives: Processing, base proteins, and other constructional ingredients. *Future Foods, 8*, Article 100248. https://doi.org/10.1016/j.fufo.2023.100248

Pawar, D., Lo Presti, D., Silvestri, S., Schena, E., & Massaroni, C. (2023). Current and future technologies for monitoring cultured meat: A review. *Food Research International, 173*, Article 113464. https://doi.org/10.1016/j.foodres.2023.113464

Plattner, B. J., Hong, S., Li, Y., Talavera, M. J., Dogan, H., Plattner, B. S., & Alavi, S. (2024). Use of pea proteins in high-moisture meat analogs: Physicochemical properties of raw formulations and their texturization using extrusion. *Foods, 13*(8), 1195. https://doi.org/10.3390/foods13081195

Pöri, P., Aisala, H., Liu, J., Lille, M., & Sozer, N. (2023). Structure, texture, and sensory properties of plant-meat hybrids produced by high-moisture extrusion. *Lebensmittel-Wissenschaft & Technologie, 173*, Article 114345. https://doi.org/10.1016/j.lwt.2022.114345

Post, M. J., Levenberg, S., Kaplan, D. L., Genovese, N., Fu, J., Bryant, C. J., Negowetti, N., Verzijden, K., & Moutsatsou, P. (2020). Scientific, sustainability and regulatory challenges of cultured meat. *Nature Food, 1*(7), 403–415. https://doi.org/10.1038/s43016-020-0112-z

Riquelme-Guzmán, C., Stout, A. J., Kaplan, D. L., & Flack, J. E. (2024). Unlocking the potential of cultivated meat through cell line engineering. *iScience, 27*(10), Article 110877. https://doi.org/10.1016/j.isci.2024.110877

Rubio, N. R., Xiang, N., & Kaplan, D. L. (2020). Plant-based and cell-based approaches to meat production. *Nature Communications, 11*(1), 6276. https://doi.org/10.1038/s41467-020-20061-y

Rueda, O., & Scherer, L. A. (2023). Frontiers 2023. What's cooking? An assessment of the potential impacts of selected novel alternatives to conventional animal products. et al. *United Nations Environment Programme*. https://doi.org/10.59117/20.500.11822/44236

Sägesser, C., Kallfelz, J. M., Boulos, S., Dumpler, J., Böcker, L., Mair, T., Nyström, L., & Mathys, A. (2024). Structurability of microalgae, soy and pea protein for extruded high-moisture meat analogues. *Food Hydrocolloids, 156*, Article 110290. https://doi.org/10.1016/J.FOODHYD.2024.110290

Santos, M. dos, Rocha, D. A. da, Bernardinelli, O. D., Oliveira Júnior, F. D., de Sousa, D. G., Sabadini, E., da Cunha, R. L., Trindade, M. A., & Pollonio, M. A. R. (2022). Understanding the performance of plant protein concentrates as partial meat substitutes in hybrid meat emulsions. *Foods, 11*(21), 3311. https://doi.org/10.3390/foods11213311

Saricay, Y., Wierenga, P. A., & de Vries, R. (2014). Changes in protein conformation and surface hydrophobicity upon peroxidase-catalyzed cross-linking of Apo-α-lactalbumin. *Journal of Agricultural and Food Chemistry, 62*(38), 9345–9352. https://doi.org/10.1021/jf502664q

Schiermeier, Q. (2019). Eat less meat: UN climate-change report calls for change to human diet. *Nature, 572*(7769), 291–292. https://doi.org/10.1038/d41586-019-02409-7

Schmid, E., Farahnaky, A., Adhikari, B., & Torley, P. J. (2022). High moisture extrusion cooking of meat analogs: A review of mechanisms of protein texturization. *Comprehensive Reviews in Food Science and Food Safety, 21*(6), 4573–4609. https://doi.org/10.1111/1541-4337.13030

Schreuders, F. K. G., Sagis, L. M. C., Bodnár, I., Erni, P., Boom, R. M., & van der Goot, A. J. (2021). Mapping the texture of plant protein blends for meat analogues. *Food Hydrocolloids, 118*. https://doi.org/10.1016/J.FOODHYD.2021.106753

Shanthakumar, P., Klepacka, J., Bains, A., Chawla, P., Dhull, S. B., & Najda, A. (2022). The current situation of pea protein and its application in the food industry. *Molecules, 27*(16), 5354. https://doi.org/10.3390/MOLECULES27165354

Shen, Y., Hong, S., Du, Z., Chao, M., O'Quinn, T., & Li, Y. (2022). Effect of adding modified pea protein as functional extender on the physical and sensory properties of beef patties. *Lebensmittel-Wissenschaft & Technologie, 154*, Article 112774. https://doi.org/10.1016/j.lwt.2021.112774

Singh, A., Tulbek, M. C., Izydorczyk, M., & Koksel, F. (2025). High moisture extrusion texturization of air-classified barley protein for the production of novel plant-based meat analogues. *Food and Bioprocess Technology, 18*(2), 1857–1872. https://doi.org/10.1007/s11947-024-03549-z

Smetana, S., Ristic, D., Pleissner, D., Tuomisto, H. L., Parniakov, O., & Heinz, V. (2023). Meat substitutes: Resource demands and environmental footprints. *Resources, Conservation and Recycling, 190*, Article 106831. https://doi.org/10.1016/j.resconrec.2022.106831

Snel, S. J. E., Amroussi, Y., van der Goot, A. J., & Beyrer, M. (2023). Rework potential of soy and pea protein isolates in high-moisture extrusion. *Foods, 12*(13), 2543. https://doi.org/10.3390/foods12132543

Stable Micro Systems Ltd.. (2023). Comparison of uniaxial extensibility of chewing gum bones. Texture analyser application study. In *Exponent connect software education Zone* (Issue REF: GUM6/TG) http://www.stablemicrosystems.com/.

Sui, X., Zhang, T., Zhang, X., & Jiang, L. (2024). High-Moisture extrusion of plant proteins: Fundamentals of texturization and applications. *Annual Review of Food Science and Technology, 15*(1), 125–149. https://doi.org/10.1146/annurev-food-072023-034346

Sun, X. D., & Arntfield, S. D. (2012). Gelation properties of myofibrillar/pea protein mixtures induced by transglutaminase crosslinking. *Food Hydrocolloids, 27*(2), 394–400. https://doi.org/10.1016/j.foodhyd.2011.11.001

Sun, D., Wu, M., Zhou, C., & Wang, B. (2022). Transformation of high moisture extrusion on pea protein isolate in melting zone during: From the aspects of the rheological property, physicochemical attributes and modification mechanism. *Food Hydrocolloids, 133*, Article 108016. https://doi.org/10.1016/j.foodhyd.2022.108016

Surya Ulhas, R., Ravindran, R., Malaviya, A., Priyadarshini, A., Tiwari, B. K., & Rajauria, G. (2023). A review of alternative proteins for vegan diets: Sources,

physico-chemical properties, nutritional equivalency, and consumer acceptance. *Food Research International, 173*, Article 113479. https://doi.org/10.1016/j.foodres.2023.113479

Totosaus, A., Montejano, J. G., Salazar, J. A., & Guerrero, I. (2002). A review of physical and chemical protein-gel induction. *International Journal of Food Science and Technology, 37*(6), 589–601. https://doi.org/10.1046/j.1365-2621.2002.00623.x

Varejão, N., & Reverter, D. (2023). *Using intrinsic fluorescence to measure protein stability upon thermal and chemical denaturation*. https://doi.org/10.1007/978-1-0716-2784-6_16

Villacís-Chiriboga, J., Sharifi, E., Elíasdóttir, H. G., Huang, Z., Jafarzadeh, S., & Abdollahi, M. (2025). Hybrid plant-based meat alternatives structured via co-extrusion: A review. *Trends in Food Science & Technology, 160*, Article 105013. https://doi.org/10.1016/j.tifs.2025.105013

Wang, J., Kadyan, S., Ukhanov, V., Cheng, J., Nagpal, R., & Cui, L. (2022a). Recent advances in the health benefits of pea protein (Pisum sativum): Bioactive peptides and the interaction with the gut microbiome. *Current Opinion in Food Science, 48*, Article 100944. https://doi.org/10.1016/J.COFS.2022.100944

Wang, Y., & Selomulya, C. (2022b). Food rheology applications of large amplitude oscillation shear (LAOS). *Trends in Food Science & Technology, 127*, 221–244. https://doi.org/10.1016/j.tifs.2022.05.018

Wang, Y., Tuccillo, F., Lampi, A., Knaapila, A., Pulkkinen, M., Kariluoto, S., Coda, R., Edelmann, M., Jouppila, K., Sandell, M., Piironen, V., & Katina, K. (2022c). Flavor challenges in extruded plant-based meat alternatives: A review. *Comprehensive Reviews in Food Science and Food Safety, 21*(3), 2898–2929. https://doi.org/10.1111/1541-4337.12964

Warner, R. D. (2019). Review: Analysis of the process and drivers for cellular meat production. *Animal, 13*(12), 3041–3058. https://doi.org/10.1017/S1751731119001897

Webb, D., Plattner, B. J., Donald, E., Funk, D., Plattner, B. S., & Alavi, S. (2020). Role of chickpea flour in texturization of extruded pea protein. *Journal of Food Science, 85*(12), 4180–4187. https://doi.org/10.1111/1750-3841.15531

Xia, Y., Zhu, L., Wu, G., Liu, T., Li, X., Wang, X., & Zhang, H. (2022). Comparative study of various methods used for bitterness reduction from pea (pisum sativum L.) protein hydrolysates. *Lebensmittel-Wissenschaft & Technologie, 159*, Article 113228. https://doi.org/10.1016/j.lwt.2022.113228

Xiang, L., Zhu, W., Jiang, B., Chen, J., Zhou, L., & Zhong, F. (2023). Volatile compounds analysis and biodegradation strategy of beany flavor in pea protein. *Food Chemistry, 402*, Article 134275. https://doi.org/10.1016/j.foodchem.2022.134275

Xiao, R., Flory, J., Alavi, S., & Li, Y. (2025). Physicochemical and functional properties of plant proteins before and after extrusion texturization. *Food Hydrocolloids, 163*, Article 111119. https://doi.org/10.1016/j.foodhyd.2025.111119

Yazar, G., Caglar Duvarci, O., Yildirim Erturk, M., & Kokini, J. L. (2019). LAOS (large amplitude oscillatory shear). *Applications for Semisolid Foods*, 97–131. https://doi.org/10.1007/978-3-030-27134-3_4

Yu, X., Yue, M., Zhang, S., Li, T., Zhang, D., Wang, X., Zhao, Y., Wu, J., Wang, C., & Ma, C. (2025). Physicochemical and structural properties of novel cornmeal, pea protein isolate and wheat gluten meat analogues prepared by high moisture extrusion. *Food Science and Biotechnology, 34*(6), 1401–1411. https://doi.org/10.1007/s10068-024-01756-0

Zang, Y., Wang, S., Gao, Y., Sun, C., Zhao, Y., Cao, Y., Lu, W., Zhang, Y., & Fang, Y. (2025). High moisture extrusion of pulse proteins: Texture, structure, and in vitro digestion characteristics of extrudates. *Food Hydrocolloids, 159*, Article 110676. https://doi.org/10.1016/j.foodhyd.2024.110676

Zhang, X., Shen, A., Zhang, Z., Zhang, T., Jiang, L., Zhou, W., Zhang, Y., & Sui, X. (2024a). Advancing molecular understanding in high moisture extrusion for plant-based meat analogs: Challenges and perspectives. *Food Chemistry, 460*, Article 140458. https://doi.org/10.1016/j.foodchem.2024.140458

Zhang, Y., Wang, Y., Zhang, R., Yu, J., Gao, Y., & Mao, L. (2022a). Tuning the rheological and tribological properties to simulate oral processing of novel high internal phase oleogel-in-water emulsions. *Food Hydrocolloids, 131*, Article 107757. https://doi.org/10.1016/j.foodhyd.2022.107757

Zhang, Y., & Xiao, Z. (2025a). *Surface Hydrophobicity*, 279–286. https://doi.org/10.1007/978-1-0716-4272-6_21

Zhang, J., Yuan, J., Han, X., Li, Q., Liao, X., & Zhao, J. (2025b). Development and characterization of fibrous high moisture extrudates based on pea protein isolate and whey protein. *Journal of the Science of Food and Agriculture, 105*(2), 760–768. https://doi.org/10.1002/jsfa.13866

Zhang, X., Zhang, Z., Shen, A., Zhang, T., Jiang, L., El-Seedi, H., Zhang, G., & Sui, X. (2024b). Legumes as an alternative protein source in plant-based foods: Applications, challenges, and strategies. *Current Research in Food Science, 9*, Article 100876.

Zhang, X., Zhao, Y., Zhang, T., Zhang, Y., Jiang, L., & Sui, X. (2022b). High moisture extrusion of soy protein and wheat gluten blend: An underlying mechanism for the formation of fibrous structures. *Lebensmittel-Wissenschaft & Technologie, 163*. https://doi.org/10.1016/j.lwt.2022.113561

Zhao, Y.-R., Peng, N., Li, Y.-Q., Liang, Y., Guo, Z.-W., Wang, C.-Y., Wang, Z.-Y., Wang, C., & Ren, X. (2024). Physicochemical properties, structural characteristics and protein digestibility of pea protein-wheat gluten composited meat analogues prepared via high-moisture extrusion. *Food Hydrocolloids, 156*, Article 110283. https://doi.org/10.1016/j.foodhyd.2024.110283

Zhu, X., Tan, B., Li, K., Liu, S., Gu, Y., Xia, T., Bai, Y., Wang, P., & Wang, R. (2022). The impacts of different pea protein isolate levels on functional, instrumental and textural quality parameters of duck meat batters. *Foods, 11*(11), 1620. https://doi.org/10.3390/foods11111620